

Resource Variation Within and Between Patches: Where Exploitation Competition, Local Adaptation, and Kin Selection Meet

Max Schmid,^{1,2} Claus Rueffler,³ Laurent Lehmann,¹ and Charles Mullan^{1,*}

1. Department of Ecology and Evolution, University of Lausanne, 1015 Lausanne, Switzerland; 2. Department of Biology, University of Tübingen, 72076 Tübingen, Germany; 3. Department of Ecology and Genetics, Animal Ecology, Uppsala University, 75236 Uppsala, Sweden

Submitted October 3, 2022; Accepted July 14, 2023; Electronically published November 17, 2023

Online enhancements: supplemental PDF.

ABSTRACT: In patch- or habitat-structured populations, different processes can favor adaptive polymorphism at different scales. While spatial heterogeneity can generate spatially disruptive selection favoring variation between patches, local competition can lead to locally disruptive selection promoting variation within patches. So far, almost all theory has studied these two processes in isolation. Here, we use mathematical modeling to investigate how resource variation within and between habitats influences the evolution of variation in a consumer population where individuals compete in finite patches connected by dispersal. We find that locally and spatially disruptive selection typically act in concert, favoring polymorphism under a wider range of conditions than when in isolation. But when patches are small and dispersal between them is low, kin competition inhibits the emergence of polymorphism, especially when the latter is driven by local competition for resources. We further use our model to clarify what comparisons between trait and neutral genetic differentiation (Q_{ST}/F_{ST} comparisons) can tell about the nature of selection. Overall, our results help us understand the interaction between two major drivers of polymorphism: locally and spatially disruptive selection, and how this interaction is modulated by the unavoidable effects of kin selection under limited dispersal.

Keywords: evolutionary branching, local adaptation, frequency-dependent selection, limited gene flow, polymorphism.

Introduction

Adaptation to exploit different resources has long been recognized as one of the major drivers of phenotypic diversity (Skúlason and Smith 1995; Smith and Skúlason 1996). One example of such resource-driven diversity can

be found in the three-spined stickleback, *Gasterosteus aculeatus*, which has diverged between lake and stream habitats in multiple locations. Across locations, lake sticklebacks have additional and longer gill rakers, allowing them to capture zooplankton, whereas stream sticklebacks have fewer and shorter rakers that are more suitable for feeding on benthic macroinvertebrates (Hendry et al. 2002; Berner et al. 2010; Ravinet et al. 2013). Another emblematic example comes from Darwin's ground finches, *Geospiza*. Within the same island, different species of this genus show highly diverged beak morphologies, with each form fitting to a specific resource: large-beaked finches are specialized on large and hard seeds, while small- and pointed-beaked finches are specialized on smaller and softer food sources (Grant and Grant 2002, 2008).

The examples of three-spined stickleback and Darwin's finches in fact each illustrate one main pathway that has been proposed to lead to adaptive polymorphism in consumer traits. Where resources vary between habitats—for instance, when lakes and streams offer different resources—diversity is driven by “spatially disruptive selection,” as different traits are favored in different locations. In this case, polymorphism leads to local adaptation, where each morph shows a better fit to the habitat it lives in (Haldane 1948; Kawecki and Ebert 2004; Leimu and Fischer 2008; Hereford 2009). In contrast, when resources vary within habitats—for instance, when each island offers a wide range of seeds—diversification is driven by local competition. This leads to character displacement owing to negative frequency-dependent selection, as individuals feeding on food sources different from others enjoy less intense competition (Maynard Smith 1962; Rosenzweig 1978; Dieckmann and Doebeli 1999; Rueffler et al. 2006a). To contrast with spatially

* Corresponding author; email: charles.mullan@unil.ch.

ORCID: Schmid, <https://orcid.org/0000-0001-7197-4775>; Rueffler, <https://orcid.org/0000-0001-9836-2752>; Lehmann, <https://orcid.org/0000-0001-9549-9577>; Mullan, <http://orcid.org/0000-0002-9875-4227>.

disruptive selection, we will refer to such selection favoring polymorphism due to local competition as “locally disruptive selection.”

Mathematical models have been useful to understand how spatially (e.g., Levene 1953; Felsenstein 1976; Brown and Pavlovic 1992; Meszéna et al. 1997; Geritz and Kisdi 2000; Svardal et al. 2015) and locally (e.g., MacArthur and Levins 1967; Roughgarden 1976; Christiansen and Loeschcke 1980; Slatkin 1980; Abrams 1986; Meszéna et al. 1997; Geritz et al. 1998; Day 2000, 2001; Ajar 2003; Rueffler et al. 2006b; Abrams et al. 2008) disruptive selection can lead to trait diversity within and between species. One salient point from these models is that dispersal and gene flow between habitats have antagonistic effects on polymorphism. On the one hand, limited dispersal favors the emergence of polymorphism under spatially disruptive selection, as it allows different morphs to become associated with different habitats (Levene 1953; Felsenstein 1976; Lenormand 2002). On the other hand, limited dispersal inhibits polymorphism when driven by locally disruptive selection because it leads to interactions among kin that are not sufficiently diverged to escape local competition (Day 2001; Ajar 2003). Put differently, polymorphism here is inhibited by kin selection, which occurs whenever a trait expressed by a focal individual affects the fitness of others that are genetically related to the focal at the loci determining the trait (Hamilton 1964; Michod 1982; Frank 1998; Rousset 2004).

Current models of consumer polymorphism have almost exclusively focused on either spatially or locally disruptive selection (citations in preceding paragraph), in effect assuming that resources vary only between or only within patches (for analyses combining spatially and locally disruptive selection but ignoring kin selection, see Day 2000; Rettelbach et al. 2013). More realistically, though, variation occurs both between and within patches, leading to both selective forces acting simultaneously. Given the antagonistic effects of dispersal on spatially and locally disruptive selection, the outcome of the evolutionary dynamics in this case is unclear. To investigate this, we model the evolution of a consumer trait when resources vary within and between patches of finite size that are connected by limited dispersal. Our results suggest that spatially and locally disruptive selection may in fact often work together to promote the emergence and maintenance of polymorphism in consumer traits.

The Model

Population and Life Cycle Events

We consider an asexual population that is divided among a large (ideally infinite) number of heterogeneous patches and that is censused at discrete demographic time points

(henceforth referred to as “years,” but the model applies to any time period that the species under consideration needs to complete its life cycle). At the beginning of each year, all patches carry the same number n of adult individuals but differ according to the resources they hold (we detail this in the next section). The following events then unfold within a year, determining the life cycle (fig. 1a): (1) resource consumption and reproduction—within each patch, adults first consume local resources and then reproduce clonally, making a large number of offspring (how consumption is modeled is specified in the next section); (2) dispersal—each offspring either remains in its natal patch (with probability $1 - m$) or disperses to another randomly sampled patch (with probability $m > 0$); (3) survival—each adult survives or dies (with probabilities γ and $1 - \gamma$, respectively), in the latter case freeing up a breeding spot or territory within its patch; and finally (4) population regulation—philopatric and immigrant offspring compete locally for open spots to become adults, so that by the end of the year each patch again carries n adult individuals.

Resource Distribution and Consumption

Ecological Variation Within and Between Patches. We assume that individuals consume a resource that varies in some relevant quantitative property within and between patches (e.g., corolla length, prey running speed). To describe this variation, we let $\mathbf{q} = \{q_1, q_2, \dots, q_{m_R}\}$ denote the set of possible values the resource can take, where $q_j \in \mathbb{R}$ is the value of the j th resource type (e.g., if the resource can take two values—say, $q_1 = 2$ and $q_2 = 4$ —then $\mathbf{q} = \{2, 4\}$). Before consumption, a patch is then characterized by a frequency distribution over \mathbf{q} (e.g., the frequency of resource of type $q_1 = 2$ could be 0.2, while that of type $q_2 = 4$ would then be 0.8). We assume that there is a finite number of such possible frequency distributions and let $\Pi_s = \{\pi_{1|s}, \pi_{2|s}, \dots\}$ stand for the s th such frequency distribution over the resource values where $\pi_{j|s}$ is the frequency of a resource of type j in a patch characterized by this s th frequency distribution (in the above example, $\pi_{1|s} = 0.2$ and $\pi_{2|s} = 0.8$). We say that a patch is in state $s \in \Omega$ if its resource distribution is Π_s and denote by π_s the frequency of patches in state s (i.e., $\sum_{s \in \Omega} \pi_s = 1$; e.g., if 30% of patches are characterized by frequencies $\pi_{1|s} = 0.2$ and $\pi_{2|s} = 0.8$, respectively, while the rest of the patches have equal frequencies of both resource types, then $\pi_1 = 0.3$ and $\pi_2 = 0.7$ with $\Pi_1 = \{0.2, 0.8\}$, $\Pi_2 = \{0.5, 0.5\}$, and $\Omega = \{1, 2\}$). The set of patches that are in the same state s belong to the same habitat type.

A patch in state s thus has resources with average property $\bar{q}_s = \sum_{j=1}^{m_R} q_j \pi_{j|s}$ and within-patch variance

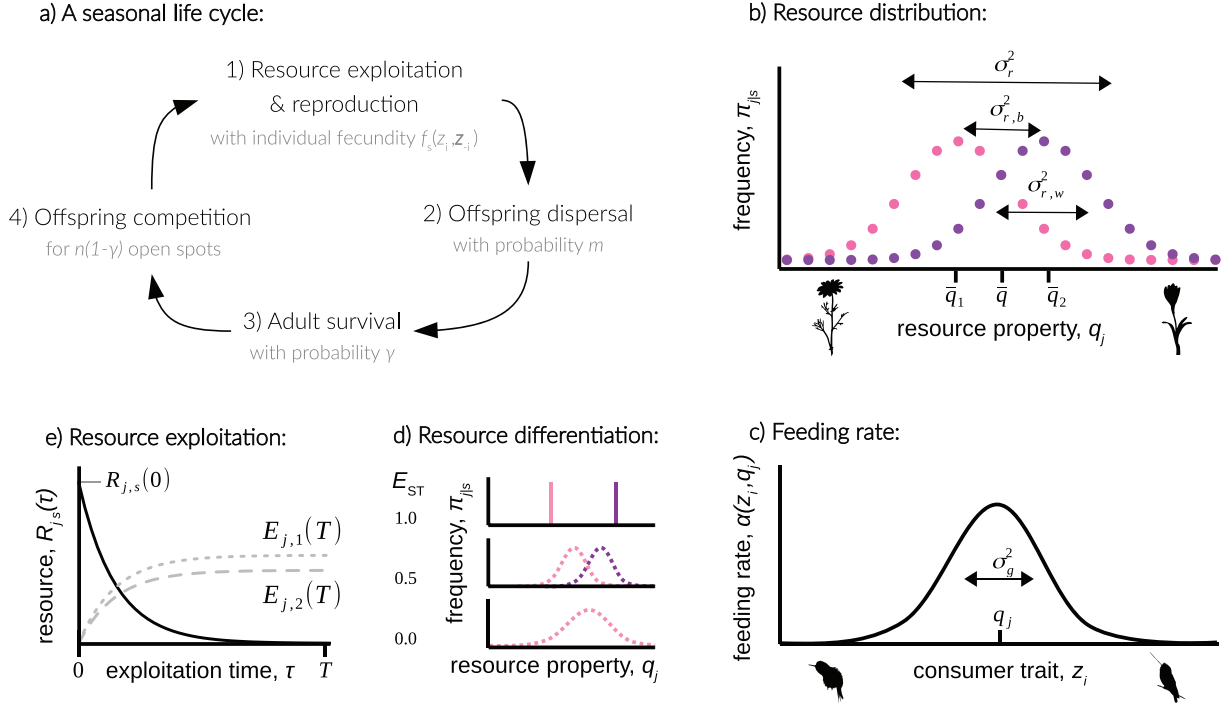


Figure 1: A model of resource exploitation for a spatially structured population. *a*, Sequence of life cycle events within each year (for details, see section “Population and Life Cycle Events”). *b*, Resource distribution $\pi_{j,s}$ within patches for two types, $s = 1$ (pink) and $s = 2$ (purple). Resources vary both within ($\sigma_{r,w}^2$) and between ($\sigma_{r,b}^2$) patches (section “Ecological Variation Within and Between Patches,” eq. [1]). *c*, Feeding rate $\alpha(z_i, q_j)$ of individual i on resources of type j with property q_j as a function of consumer trait z_i (eq. [3]), which is maximal when the trait value matches the resource property, $z_i = q_j$. *d*, Resource differentiation among patches E_{ST} (eq. [2]) for different resource distributions $\pi_{j,s}$ within patches of two types, $s = 1$ (pink) and $s = 2$ (purple). When $E_{ST} = 1$, the two habitats contain a single different resource; when $E_{ST} = 0$, there is a single habitat offering a range of resources. *e*, Within-year resource dynamics according to equation (I.A) in box 1 with the amount $R_{j,s}(\tau)$ of resource j in a patch of type s in black and the energy $E_{1,s}(\tau)$ (gray short-dashed line) and $E_{2,s}(\tau)$ (gray long-dashed line) accumulated by two individuals where individual 1 expresses a trait that allows extraction of more resources at the expense of individual 2. The two birds and plants in *b* and *c* were published under the CC0 1.0 license at <https://phylopic.org>.

$\sigma_{r,w,s}^2 = \sum_{j=1}^{n_R} (q_j - \bar{q}_s)^2 \pi_{j,s}$. At the global level, the resource has an average value $\bar{q} = \sum_{s \in \Omega} \pi_s \bar{q}_s$ and variance

$$\sigma_r^2 = \sum_{s \in \Omega} \sum_{j=1}^{n_R} (q_j - \bar{q})^2 \pi_{j,s} \pi_s = \sigma_{r,w}^2 + \sigma_{r,b}^2, \quad (1)$$

which can be decomposed into the average within-patch resource variance, $\sigma_{r,w}^2 = \sum_{s \in \Omega} \sigma_{r,w,s}^2 \pi_s$, and the variance among patch means, $\sigma_{r,b}^2 = \sum_{s \in \Omega} (\bar{q}_s - \bar{q})^2 \pi_s$ (fig. 1*b*). This decomposition allows us to quantify the level of resource differentiation among patches with

$$E_{ST} = \frac{\sigma_{r,b}^2}{\sigma_{r,b}^2 + \sigma_{r,w}^2}, \quad (2)$$

which denotes the proportion of resource variance that is due to variance between patches (fig. 1*d*). When $E_{ST} = 1$, all resource variation is between patches (fig. 1*d*, *top*), where it is only within patches when $E_{ST} = 0$ (fig. 1*d*, *bottom*).

Trait-Based Competition for Resources. Each year, individuals consume local resources within their patch (step 1 in section “Population and Life Cycle Events”). We assume that their ability to consume these resources depends on a quantitative trait they express. For instance, the ability of a hummingbird to extract nectar depends on how well the length of its bill matches the length of the corolla tube of the flowers it visits. To capture such a situation or, more generally, a scenario of trait-based resource consumption, we let the rate at which an individual indexed as $i \in \{1, 2, \dots, n\}$ (recall that n is the number of adults in a patch) feeds on a resource of type j be

$$\alpha(z_i, q_j) = \exp\left(-\frac{(z_i - q_j)^2}{2\sigma_g^2}\right), \quad (3)$$

where $z_i \in \mathbb{R}$ is the value of the relevant trait expressed by this individual. According to equation (3), the feeding rate of an individual on resource j is maximal when its trait value

Box 1: Dynamics of within-year resource consumption

To determine the amount of resources an individual consumes within a year, we assume that adults feed over a time interval of length T (taking place within step 1 of the life cycle; see section “Population and Life Cycle Events”). The variable T thus controls how much time individuals have available to consume resources within a year. If we denote by $R_{j,s}(\tau)$ the abundance of resource j in a patch of type s at time τ ($0 \leq \tau \leq T$) and by $E_{i,s}(\tau)$ the energy accumulated by individual i via consumption in that patch at time τ , then these variables change according to

$$\frac{dR_{j,s}(\tau)}{d\tau} = -R_{j,s}(\tau) \sum_{k=1}^n \alpha(z_k, q_j) \quad \text{for } j \in \{1, 2, \dots, n_R\}, \quad (\text{I.Aa})$$

$$\frac{dE_{i,s}(\tau)}{d\tau} = \beta \sum_{j=1}^{n_R} R_{j,s}(\tau) \alpha(z_i, q_j) \quad \text{for } i \in \{1, 2, \dots, n\}, \quad (\text{I.Ab})$$

where β is the energy content per resource unit, which is assumed to be the same for all resources, and n_R is the number of resource types. Individuals with a higher feeding rate $\alpha(z_i, q_j)$ thus accumulate more resources of type j at the expense of other individuals in the patch (fig. 1e). The quantity of a resource j at the beginning of each year is determined by the state s of the patch, that is, by

$$R_{j,s}(0) = R\pi_{j|s}, \quad (\text{I.B})$$

where R is the total amount of resources, which is assumed to be the same in all patches. Resources are thus brought back to a common value R each year. The energy budget of each individual is initially zero, $E_{i,s}(0) = 0$. Equation (I.A) can be solved to obtain the net energy uptake $E_{i,s}(T)$ that an individual i has accumulated by time T . In fact, the net energy uptake of individual i in a focal patch of type s obtained from resource j can be written as

$$E_{i,s}(T) = E_s(z_i, \mathbf{z}_{-i}) = \beta \sum_{j=1}^{n_R} \left[R_{j,s}(0) \left(1 - \exp\left(-T \sum_{k=1}^n \alpha(z_k, q_j)\right) \right) \right] \frac{\alpha(z_i, q_j)}{\sum_{k=1}^n \alpha(z_k, q_j)}, \quad (\text{I.C})$$

which we denote by $E_s(z_i, \mathbf{z}_{-i})$ to highlight that the energy uptake of an individual depends on its trait z_i and on the collection $\mathbf{z}_{-i} = (z_1, z_2, \dots, z_{i-1}, z_{i+1}, \dots, z_n)$ of traits expressed by its $n - 1$ patch neighbors. The term within square brackets in equation (I.C) corresponds to the total amount of resource j that is consumed within a time period in a patch that is in state s . As the exploitation time increases (i.e., as $T \rightarrow \infty$), this converges to the amount of resources available, $R_{j,s}(0)$, as individuals have sufficient time to consume all resources in the patch, and equation (I.C) reduces to equation (4).

matches the resource property, $z_i = q_j$, and declines with increasing distance between z_i and q_j , with the rate of decline inversely related to σ_g^2 (fig. 1c). The parameter σ_g^2 thus describes to what extent individuals can be generalists: an individual with trait z_i can feed at a high rate on a wider range of resource types when σ_g^2 is large compared with when σ_g^2 is small.

We develop in box 1 an explicit within-year dynamical model of resource consumption, where individuals compete for each resource of type j according to their consumption rate $\alpha(z_i, q_j)$. Assuming that the time dedicated to consumption each year is sufficient for all resources to be consumed, we obtain from this model that the energy $E_s(z_i, \mathbf{z}_{-i})$ that a focal individual with

trait z_i obtains in patch of type s when its $n - 1$ patch neighbors express the collection of phenotypes $\mathbf{z}_{-i} = (z_1, z_2, \dots, z_{i-1}, z_{i+1}, \dots, z_n)$ is

$$E_s(z_i, \mathbf{z}_{-i}) = \beta R \sum_{j=1}^{n_R} \pi_{j|s} \frac{\alpha(z_i, q_j)}{\sum_{k=1}^n \alpha(z_k, q_j)}, \quad (4)$$

where $\beta > 0$ is the energy content per resource unit (assumed to be identical for all resources) and $R > 0$ is the total abundance of resources per patch (assumed to be the same in all patches). The term within the sum of equation (4) is the relative amount of resource of type j that the focal individual accumulates. This amount is proportional to the ratio $\alpha(z_i, q_j) / \sum_{k=1}^n \alpha(z_k, q_j)$, which

captures the success of the focal relative to its neighbors in the contest for resources. In a patch where individuals all express the same trait z , each obtains the same share $1/n$, but this share increases for the focal if its trait is better adapted to consume resource j than the trait of others. In fact, equation (4) corresponds to what is referred to as a contest success function of the ratio type (Hirshleifer 1989), here summed over the contests for all resource types j .

Fecundity, Fitness, and Evolutionary Dynamics

We assume that the fecundity of an individual (the total number of offspring it produces during step 2 of the life cycle) is proportional to the total energy it has accumulated; that is, the fecundity of individual i with trait z_i in a patch in state s and where its neighbors have traits \mathbf{z}_{-i} is given by

$$f_s(z_i, \mathbf{z}_{-i}) = kE_s(z_i, \mathbf{z}_{-i}), \tag{5}$$

where k is the conversion factor from energy to offspring (assuming that energy maps to fecundity by some other monotonically increasing function would not change qualitatively our results). Note that equations (4) and (5) entail that the same total number of offspring is produced in each patch (i.e., the sum of $f_s(z_i, \mathbf{z}_{-i})$ over all i is equal to $k\beta R$ for all s). In other words, selection is “soft” (Wallace 1975; Christiansen 1975; Débarre and Gandon 2011). This is because equation (4) assumes that the consumption period is long enough for all resources to be consumed each year in each patch. We relax this assumption later. From fecundity as given by equation (5), we can characterize an individual’s fitness, which here is defined as the expected number of successful offspring produced by this individual over one full year (those that establish as adults, including itself if it survives). Thus, while fecundity is influenced by local adaptation and resource competition, fitness is additionally affected by competition for breeding spots in each patch. The individual fitness measure, which we detail in section S1.1 of the supplemental PDF, lays the basis of our evolutionary analysis.

We are interested in the genetic evolution of the consumer trait z , in particular whether gradual evolution can result in polymorphism. Our approach is based on the second-order sensitivity analysis of invasion fitness performed in Ohtsuki et al. (2020). We assume that mutations are rare with small phenotypic effect such that evolutionary dynamics occur in two steps. First, the population evolves gradually under directional selection via the recurrent input of mutations. The population eventually converges to a singular phenotype, denoted as z^* , where directional selection ceases to act. Once the population expresses z^* , it either experiences stabilizing se-

lection and remains monomorphic (fig. 2e) or experiences disruptive selection and becomes polymorphic (fig. 2f). The process of transitioning from a monomorphic to a dimorphic phenotype distribution is referred to as “evolutionary branching” (Geritz et al. 1998).

Our analysis of selection is described in section S2 of the supplemental PDF. It allows us to characterize directional (eq. [S19]) and disruptive (eqq. [S33], [S34]) selection on traits in terms of their effects on fecundity, in populations where limited dispersal leads to interactions among relatives (under our life cycle assumptions given in section “Population and Life Cycle Events”). These general equations combine three fundamental sources of selection: (i) spatial heterogeneity (as fecundity varies with patch type), (ii) social or ecological interactions (as fecundity varies with the traits of neighbors, here due to resource competition), and (iii) kin selection (with directional and disruptive selection depending on relatedness-weighted indirect fecundity effects, with relatedness coefficients computed using standard identity-by-descent arguments; e.g., eq. [S14] in the supplemental PDF). The consequences of these different sources of selection for the evolution of the consumer trait z of our model are not straightforward because they may interact with one another. Spatial heterogeneity favors local adaptation, local exploitation competition favors character displacement within patches, and kin selection modulates these via the following two effects. First, competition among relatives (“kin competition”) leads to an overall reduction of the strength of selection acting on competitive traits (as increased fecundity comes at the expense of relatives that compete locally; Taylor 1992; Frank 1998; Rousset 2004). Second, any advantage from being locally rare, in particular owing to the exploitation of underutilized resources, tends to be short-lived under limited dispersal. This is because a mutant individual using a resource that is underutilized by the resident is likely to compete within its patch against relatives and thus against other mutants that use the same resource (i.e., a globally rare mutant is not necessarily locally rare). In this sense, kin selection tends to oppose locally disruptive selection (Day 2001; Ajar 2003). We investigate these interactions and determine the conditions under which selection leads to polymorphism in trait z in section S3 of the supplemental PDF. Our main findings are summarized below.

Results

How Resource Variation Between and Within Patches Favors Polymorphism

We find that the population first evolves toward the singular trait value

$$z^* = \bar{q}, \tag{6}$$

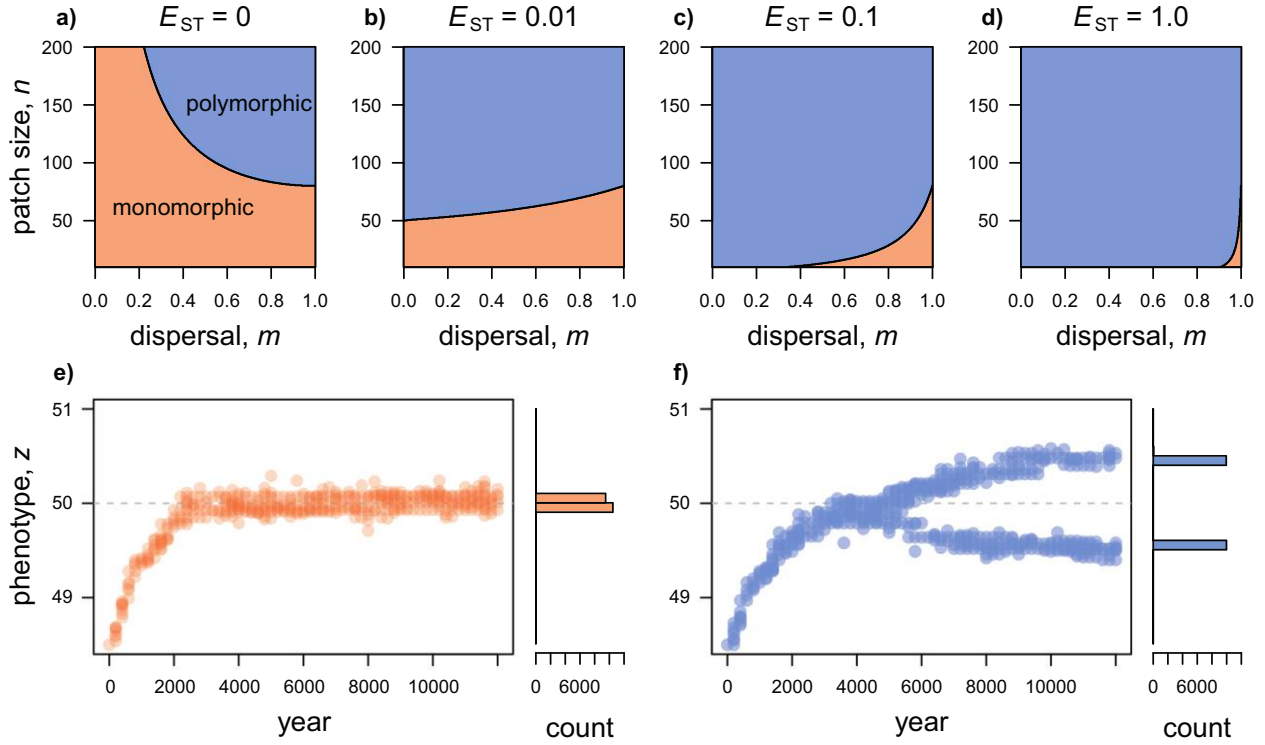


Figure 2: Evolution of polymorphism with locally and spatially varying resources. *a–d*, Parameter space in which selection is stabilizing (pink) or disruptive (blue) from condition (7) for four levels of resource differentiation: $E_{ST} = 0$ (*a*), $E_{ST} = 0.01$ (*b*), $E_{ST} = 0.1$ (*c*), and $E_{ST} = 1$ (*d*). Other parameters: $\gamma = 0$, $\sigma_r^2 = 2$, and $\sigma_g^2 = 1.95$. *e, f*, Simulated evolution of the consumer trait z when selection is stabilizing (*e*; $m = 0.9$) or disruptive (*f*; $m = 0.1$). See section S4 of the supplemental PDF for details on the simulation procedure. Other parameters: $\sigma_r^2 = 1$, $E_{ST} = 0.25$, $n = 10$, $\gamma = 0$, and $\sigma_g^2 = 1$. Each segregating phenotype every 50 years is represented by a filled circle. The gray dashed line indicates the singular trait value $z^* = 50$. As predicted by our mathematical analysis, the population first converges to z^* and then remains monomorphic when selection is stabilizing (*e*) or becomes polymorphic when selection is disruptive (*f*).

where the consumer trait matches the average resource property (for the derivation, see sec. S3.1.2 of the supplemental PDF; in line with models based on soft selection, e.g., Geritz et al. 1998; Day 2001; Ajar 2003; Svardal et al. 2015; Ohtsuki et al. 2020). Once the population has converged to express $z^* = \bar{q}$, our analysis (sec. S3.1.3 of the supplemental PDF) shows that selection is disruptive and therefore favors the emergence of polymorphism if

$$\sigma_r^2[\chi_b E_{ST} + \chi_w(1 - E_{ST})] > \sigma_g^2, \quad (7)$$

where

$$\chi_b = \frac{2n}{1 + nm + \gamma} + \mathcal{O}(1) \quad (8a)$$

$$\chi_w = \frac{nm}{1 + nm + \gamma} + \mathcal{O}(1/n) \quad (8b)$$

are complicated nonnegative quantities that depend on demographic parameters, here shown to leading order in the limit of large patch size and low dispersal (when $n \rightarrow \infty$ and $m \rightarrow 0$, with the remainder in [8a] remain-

ing bounded and that of [8b] going to zero in this limit; for full expressions, see eqq. [S62] and [S64] in sec. S3.1.3 of the supplemental PDF).

In the limiting case of infinitely large patches and complete dispersal (such that $\chi_b \rightarrow 1$ and $\chi_w \rightarrow 1$), condition (7) reduces to the classical condition $\sigma_r^2 > \sigma_g^2$ (Slatkin 1979; Geritz et al. 1998; Dieckmann and Doebeli 1999). As in these models, polymorphism here is favored when the total resource variance σ_r^2 is larger than the degree of consumer generalism σ_g^2 . This is easy to intuit and reflects that greater resource diversity σ_r^2 provides more ecological opportunities and facilitates the coexistence of specialized consumers. In contrast, a generalist with large σ_g^2 can successfully consume a wide range of resources and thereby prevents the emergence of specialized morphs. Condition (7) generalizes this classical result, helping us understand how the interaction between resource heterogeneity with limited dispersal and finite patch size influences the condition for polymorphism. In condition (7), the total variation in resources σ_r^2 is partitioned into variation between and within patches. Both types of variation add up

to contribute to polymorphism, as the left-hand side of condition (7) can be rewritten as $\chi_b \sigma_{r,b}^2 + \chi_w \sigma_{r,w}^2$ (from eqq. [1], [2]), with variation between patches weighted by χ_b and that within patches by χ_w . We discuss these two contributions below.

Between-patch variation contributes most to disruptive selection when $\chi_b E_{ST}$ is large compared with $\chi_w (1 - E_{ST})$. If this is so and condition (7) holds, polymorphism is primarily driven by spatially disruptive selection favoring local adaptation (i.e., favoring individuals whose traits match their local resource average). Inspection of χ_b shows that it is most sensitive to dispersal m , rapidly decreasing as dispersal increases (eq. [8a]; figs. 2b–2d, 3a). This reflects the well-known notion that gene flow inhibits local adaptation as it

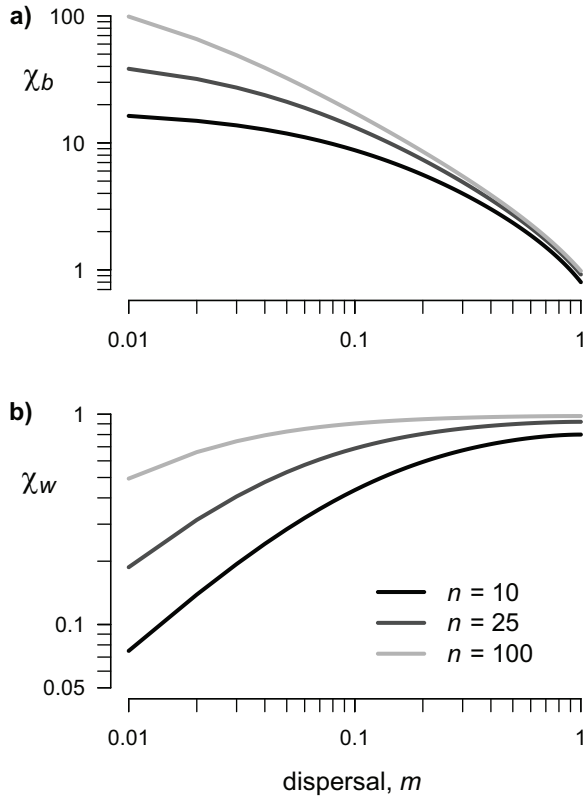


Figure 3: Disruptive selection and the weights for spatial and local resource variation in equation (9). *a*, *b*, χ_b (*a*) and χ_w (*b*) with $n = 10$ (black), 25 (dark gray), and 100 (light gray; from eqq. [S62]–[S64] in sec. S3.1.3 of the supplemental PDF). Other parameters: $\gamma = 0$. In a panmictic population ($m = 1$), both weights are equal (namely, $\chi_b = \chi_w = 1 - 2/n$) and reflect the effect of patch size on the strength of competition for resources (eq. [4]). Otherwise, $\chi_b > \chi_w$, indicating that spatial resource variation typically plays a bigger role than local variation for a given level of total resource variation (σ_r^2). While χ_b decreases, χ_w increases with dispersal, showing that spatially and locally disruptive selection are favored and disfavored, respectively, by limited dispersal.

homogenizes genetic variation between patches (e.g., Day 2000; Lenormand 2002). Furthermore, χ_b decreases as adult survival γ increases and patch size n decreases (eq. [8]; figs. 2a–2d, 3a, S1; figs. S1–S4 are available online), indicating that spatially disruptive selection is weaker when generation overlap is long and patches are small. This is because these conditions increase relatedness within patches and thus strengthen kin competition, such that an individual’s fitness increasingly comes at the expense of that of relatives. Such kin competition reduces the strength of selection on competitive traits (Taylor 1992; Frank 1998; Rousset 2004).

Conversely, within-patch resource variation contributes most to disruptive selection when $\chi_w (1 - E_{ST})$ is large compared with $\chi_b E_{ST}$. If so and condition (7) holds, polymorphism is primarily driven by locally disruptive selection or, more specifically, negative frequency-dependent disruptive selection at the local scale. This selection favors rare morphs in each patch because these morphs are able to exploit resources for which there is less intense competition locally. In contrast to χ_b , the weighting factor χ_w increases with dispersal m (eq. [9]; figs. 2a, 3b, S1 for the effect of adult survival γ and patch size n). The reason is that under weak dispersal, individuals in the same patch tend to express the same trait value, as they tend to be genetically related and, as a result, cannot easily enjoy the benefits of being locally rare (Day 2001; Ajar 2003).

Analysis of condition (7) thus reveals that dispersal m can either hinder or favor the emergence of polymorphism, depending on whether resource variation is primarily distributed between or within patches. However, even when between-patch differentiation $E_{ST} > 0$ is relatively low, limited dispersal still favors rather than hinders polymorphism (fig. 2b, 2c). This boils down to the fact that $\chi_b \geq \chi_w$ (with equality only when $m = 1$; see eq. [S65] and fig. S1a). Thus, under limited dispersal spatially disruptive selection due to between-patch variation has a greater weight than locally disruptive selection due to within-patch variation in determining whether polymorphism emerges.

Our condition (7) is in perfect agreement with previous expressions derived for less general ecological models. In particular, when resources vary only within patches ($E_{ST} = 0$) and generations do not overlap ($\gamma = 0$), we recover the polymorphism condition of Ajar (2003, his eq. [25]). When resources vary only between patches ($E_{ST} = 1$), condition (7) reduces to equation (66) of Ohtsuki et al. (2020) under high adult survival ($\gamma \sim 1$, akin to a Moran model); to $\sigma_r^2((2 - m)/m) > \sigma_g^2$ of Svoldal et al. (2015, their eq. [C.15]) under no adult survival and infinite patch size ($\gamma = 0$ and $n \rightarrow \infty$); and to equation (7) of Boussange and Pellissier (2022) under weak selection for isolation by distance (where our σ_g^2 is large, their $p = 1/(2\sigma_g^2)$ is small, and their $r = 0$). In contrast to these previous studies, our

result holds for arbitrary resource distributions both within and between habitats (in addition to allowing for limited dispersal, finite patch size, and intermediate adult survival).

Gradual Emergence of Polymorphism, Its Distribution, and Genetic Signatures

Condition (7) determines whether selection favors the emergence of polymorphism. But it does not inform us about the long-term fate of the morphs, specifically their final trait values and their distribution within and between patches. To investigate this, we ran stochastic individual-based simulations for a population occupying 2,000 patches (using Nemo-age; Cotto et al. 2020; for details, see sec. S4 of the supplemental PDF). We explore various combinations of parameters, in particular various distributions of resources within and between patches (by varying E_{ST}). As predicted by our analysis, the population first converges to match the average resource property \bar{q} while remaining largely monomorphic (fig. 2e, 2f). When condition (7) is not satisfied, the population remains monomorphic with a unimodal phenotype distribution (fig. 4a, 4b in pink). But when condition (7) is satisfied, the population becomes polymorphic with two highly differentiated morphs eventually coexisting in the population: one that specializes on “small” resources (small q values) and another that specializes on “large” resources (large q values; fig. 2f; fig. 4a, 4b in blue).

The emergence of polymorphism is typically accompanied by a significant increase in population phenotypic variance (denoted as V_p ; fig. 4c, 4d in black). The final level of phenotypic variance V_p maintained in a polymorphic population depends on gene flow and the resource distribution. When resource variation is mostly within patches (small E_{ST}), V_p increases with dispersal (fig. 4c). When resources vary primarily between patches (large E_{ST}), variance V_p decreases with dispersal (fig. 4d). This reflects how gene flow interacts differently with locally and spatially disruptive selection (as elaborated in section “How Resource Variation Between and Within Patches Favors Polymorphism”). In addition, phenotypic variance increases with E_{ST} (fig. S2). In other words, two morphs maintained by spatially disruptive selection tend to be differentiated more strongly than two morphs maintained by purely locally disruptive selection. This further supports the notion that spatially disruptive selection is a stronger driver of polymorphism than locally disruptive selection (as evident from condition [7] and eq. [8]).

To explore how the two morphs are distributed among patches, it is useful to decompose the phenotypic variance into within ($V_{p,w}$) and between ($V_{p,b}$) patch trait variance, $V_p = V_{p,w} + V_{p,b}$. As expected, within-patch phenotypic variance $V_{p,w}$ is greatest when resource variation occurs only

within patches and dispersal is high (small E_{ST} and large m ; fig. 4c in white), while between-patch phenotypic variance $V_{p,b}$ dominates when resource variation is concentrated among patches and dispersal is limited (large E_{ST} and small m ; fig. 4d in orange). This indicates that both morphs tend to co-occur in the same patch in the former case, while the different morphs tend to inhabit different patches in the latter case. Interestingly, as long as $E_{ST} > 0$, within-patch phenotypic variance responds nonmonotonically to gene flow, with $V_{p,w}$ initially increasing but ultimately decreasing with dispersal m (fig. 4d in white). This pattern can be understood by considering that when resources are differentiated between patches ($E_{ST} > 0$) and patches are isolated ($m \ll 1$), patches tend to be fixed for different phenotypes owing to local sampling effects so that $V_{p,w}$ is small. As dispersal increases, these different phenotypes start mixing within patches, leading initially to an increase in within-patch variance $V_{p,w}$. But past a threshold of dispersal, gene flow counteracts differentiation among patches, which eventually generates a decline in $V_{p,w}$ (as reported in simulation studies with $E_{ST} = 1$; e.g., McDonald and Yeaman 2018).

How gene flow and selection shape the distribution of morphs among patches can be further investigated through $Q_{ST} = V_{G,b}/(V_{G,b} + V_{G,w})$, which measures between-patch differentiation in additive genetic variance (where additive genetic variance equals phenotypic variance in our asexual model in the absence of environmental effects so that $V_{G,b} = V_{p,b}$ and $V_{G,w} = V_{p,w}$). As expected, Q_{ST} is positively related to E_{ST} , the resource differentiation between patches (fig. S3). To specify the effects of selection on phenotypic differentiation, we can compare Q_{ST} with differentiation in allele frequencies, F_{ST} , at neutral loci (e.g., Whitlock 2008; Ovaskainen et al. 2011; Leinonen et al. 2013). In addition to a locus coding for the consumer trait z , individuals in our simulations carry a neutral locus similar to a microsatellite marker at which we compute F_{ST} following the Weir-Cockerham approach (Weir and Cockerham 1984, p. 1363; for details, see sec. S4 of the supplemental PDF). Both loci are linked owing to clonal reproduction, but since many patches belong to the same habitat and dispersal is uniform, such linkage should not lead to strong associations between trait value and allelic state at the neutral marker. We also quantify neutral genetic differentiation from our analytical model via pairwise relatedness r , that is, the probability that two individuals randomly sampled without replacement from the same patch are identical by descent in a population monomorphic for the singular strategy, $z^* = \bar{q}$ (which for haploids structured according to the infinite island model corresponds to the probability that two genes sampled in two individuals sampled from the patch have coalesced in that same patch; Rousset 2004; see eq. [S17] in sec. S2.2.2 of the supplemental PDF).

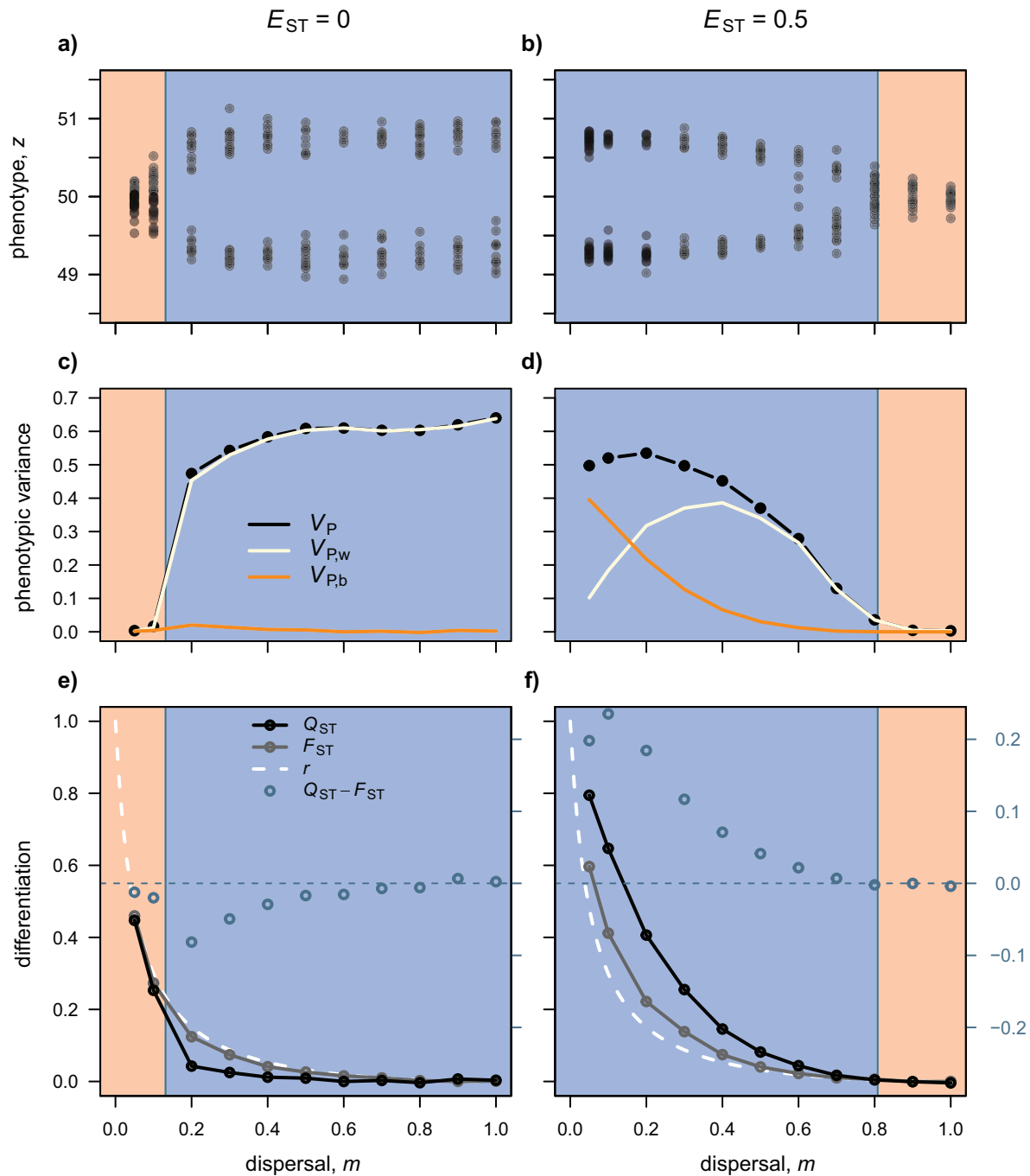


Figure 4: Distribution of polymorphism within and between patches. *a, b*, Trait values present in a simulated population after 2,000 years of evolution as a function of dispersal m with $E_{ST} = 0$ (*a*; and $\sigma_s^2 = 2$) and $E_{ST} = 0.5$ (*b*; and $\sigma_s^2 = 1$). Other parameters: $\sigma_b^2 = 1$, $\gamma = 0$, and $n = 10$. Blue and pink areas indicate levels of dispersal that lead to disruptive and stabilizing selection, respectively (from condition [7]). Simulations and mathematical analyses are thus consistent, with the population evolving to being dimorphic where selection is disruptive (blue) and monomorphic where selection is stabilizing (pink). *c, d*, Phenotypic variance in the same evolved populations as in *a* and *b* with total variance V_P in black, decomposed as variance within patches $V_{P,w}$ (white) and between patches $V_{P,b}$ (orange). Phenotypic variance is thus significantly greater when selection is disruptive (blue area). *e, f*, Phenotypic differentiation Q_{ST} (in black) versus neutral genetic differentiation quantified with F_{ST} (in gray) from simulations (using the Weir-Cockerham approach with the hierfstat package in R) and pairwise relatedness r (dashed white line) from our mathematical model (using eq. [S17]). Dark blue open circles give $Q_{ST} - F_{ST}$ with the scale given on the right-hand side, and the blue dashed line indicates $Q_{ST} = F_{ST}$. This shows that $Q_{ST} = F_{ST}$ when selection is stabilizing (pink), $Q_{ST} < F_{ST}$ when selection is locally disruptive (i.e., when $E_{ST} = 0$; blue area in *a*), and $Q_{ST} > F_{ST}$ when selection is disruptive and $E_{ST} > 0$ (blue area in *b*).

Comparing phenotypic differentiation Q_{ST} with neutral genetic differentiation (either with F_{ST} from our simulations or relatedness r from the analytical model) reveals three patterns (blue circles in fig. 4e, 4f): (i) in the absence of polymorphism, Q_{ST} equals neutral genetic differentiation (pink regions in fig. 4e, 4f); (ii) in the presence of polymorphism and resource variation among patches ($E_{ST} > 0$), Q_{ST} exceeds neutral genetic differentiation (blue region in fig. 4f); and (iii) in the presence of polymorphism and resource variation only within patches ($E_{ST} = 0$), Q_{ST} is lower than neutral genetic differentiation (blue region in fig. 4e). In other words, when the trait is under stabilizing selection for the same value in all patches so that the population is monomorphic, trait differentiation Q_{ST} is identical to F_{ST} . But when resource variation leads to polymorphism, Q_{ST} deviates from F_{ST} . Spatially disruptive selection leads to an increase in between-patch phenotypic variance $V_{p,b}$ and therefore to an increase in Q_{ST} relative to F_{ST} . Conversely, locally disruptive selection boosts within-patch phenotypic variance $V_{p,w}$, causing a drop in Q_{ST} compared with F_{ST} .

Our observation that phenotypic differentiation exceeds neutral genetic differentiation in the presence of polymorphism and resource differentiation ($E_{ST} > 0$) aligns with the common notion that $Q_{ST} > F_{ST}$ signals local adaptation (e.g., Whitlock 2008; Leinonen et al. 2013). Another common idea is that $Q_{ST} < F_{ST}$ is an indicator of stabilizing selection favoring the same trait value in all patches (i.e., under spatially uniform selection where $E_{ST} = 0$ and condition [7] does not hold; e.g., Merilä and Crnokrak 2001; McKay and Latta 2002; Leinonen et al. 2008). By contrast, we find that phenotypic differentiation is actually similar to neutral genetic differentiation in this case, $Q_{ST} = F_{ST}$ (this has also been demonstrated mathematically in Mullan and Lehmann 2019, their eq. [C26]). This is because stabilizing selection acts on both within-patch and between-patch variation. Rather, we find $Q_{ST} < F_{ST}$ when selection is disruptive due to local competition only (condition [7] holds and $E_{ST} = 0$), as this maintains greater phenotypic variation within patches than expected under neutrality (as suggested by Lamy et al. 2012).

Hard Selection and Alternative Routes to Polymorphism

Our results so far are based on equation (4), which assumes that the time dedicated to resource exploitation within a year is long such that all resources are consumed. This has the consequence that the total number of offspring born is the same in all patches. To relax this assumption, we assume here that exploitation time is short such that individuals do not interfere with one another through resource consumption (i.e., T in box 1 is small; for details, see eq. [S66] in sec. S3.2.1 of the supplemental PDF; for results based on intermediate exploitation time, see fig. S4). This has

two consequences. First, the total number of offspring born in each patch is no longer identical, as not all resources can be consumed in the time given. Instead, patches that are occupied by locally adapted individuals have a larger offspring production since its inhabitants extract more resources, allowing them to produce more offspring (leading to hard selection; for an analysis where exploitation time is short and selection is soft through an extra regulation step, in which case the condition for polymorphism is identical to that of long exploitation time and resource variation only between patches [i.e., to condition (7) with $E_{ST} = 1$], see sec. S3.2.4 of the supplemental PDF). Second, the absence of interference through resource consumption means that there cannot be any negative frequency-dependent selection within patches—that is, locally disruptive selection is absent. In what follows, selection for polymorphism is therefore exclusively driven by spatially disruptive selection. To obtain analytical results, we assume that there are two types of patches showing a high degree of symmetry: specifically, the two types of patches occur at equal frequency ($\pi_1 = \pi_2 = 1/2$), the distribution of resources within patches is Gaussian with the same variance $\sigma_{r,w}^2$, and the mean for patches of types 1 and 2 are given by $\bar{q}_1 = \bar{q} - \sigma_{r,b}$ and $\bar{q}_2 = \bar{q} + \sigma_{r,b}$, respectively, such that $\sigma_{r,b}^2$ is the variance of patch means (for details of this model, see sec. S3.2.1 of the supplemental PDF). This model can thus be seen as an extension to Meszéná et al. (1997) and Ronce and Kirkpatrick (2001), who analyzed two-patch models under hard selection for local adaptation in the absence of within-patch resource differentiation ($\sigma_{r,w}^2 = 0$ so that $E_{ST} = 1$) and of kin competition (infinite patch size $n \rightarrow \infty$).

As with long exploitation time T , we find that the trait value $z^* = \bar{q}$ that matches the average resource is a singular strategy (sec. S3.2.2 of the supplemental PDF). A numerical analysis shows that, provided between-patch resource differentiation E_{ST} is not too strong, z^* is an attractor of directional selection (fig. 5a–5c, solid colored regions). In other words, as long as patches are not too different, the population initially converges to express $z^* = \bar{q}$. In this case, selection is disruptive and leads to polymorphism when

$$\sigma_r^2(\chi_h E_{ST} - (1 - E_{ST})) > \sigma_g^2, \quad (9)$$

where $\chi_h \geq 0$ depends in a complicated manner on demographic parameters (on patch size n , dispersal probability m , and adult survival γ ; for details, see eq. [S88] in the supplemental PDF; solid pink region in fig. 5a–5c for parameter combinations where condition [9] holds). Otherwise, selection is stabilizing and the population remains fixed for $z^* = \bar{q}$ (solid blue region in fig. 5a–5c for parameter combinations where condition [9] does not hold). The factor χ_h responds to demographic parameters in the same way as χ_b (eq. [8]), except for the fact that χ_h is larger by a small

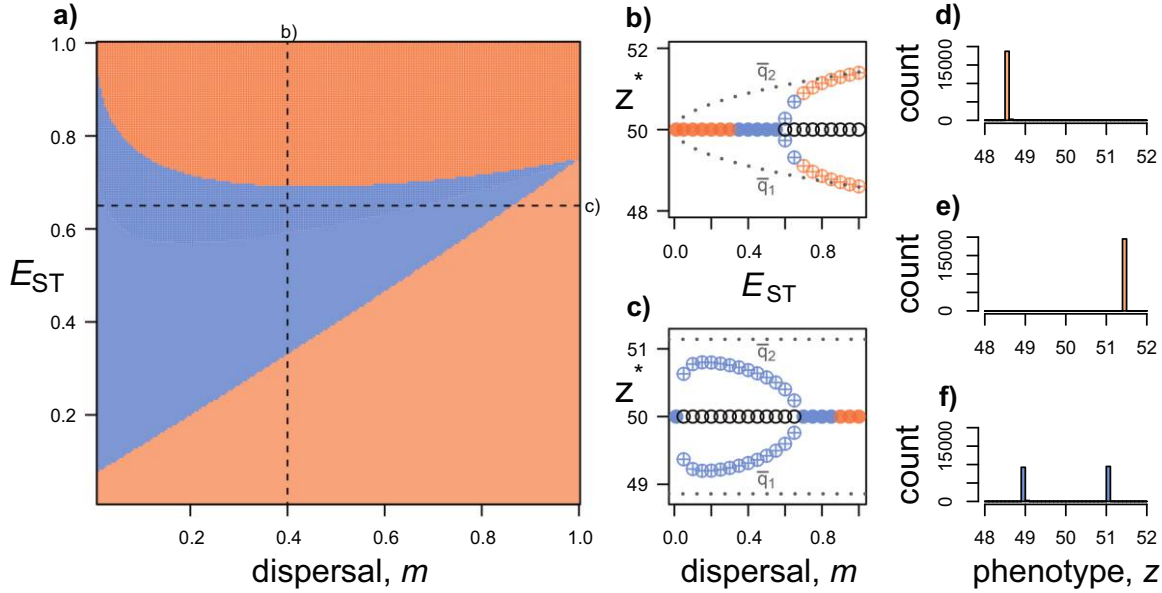


Figure 5: Evolutionary dynamics under hard selection. *a*, Combinations of resource differentiation E_{ST} and dispersal m leading to stabilizing (pink) or disruptive (blue) selection for short exploitation time so that offspring production may vary among patches (selection is hard; for details, see section “Hard Selection and Alternative Routes to Polymorphism”; for analysis, see sec. S3.2 of the supplemental PDF). Other parameters: $n = 10$, $\gamma = 0$, $\sigma_r^2 = 2$, and $\sigma_g^2 = 1$. Under stabilizing selection, the population adapts to the average resource property $z^* = \bar{q}$ (solid pink) or to one of the two habitats depending on initial conditions ($z_1^* = \bar{q} - \theta$ or $z_2^* = \bar{q} + \theta$; speckled pink). When selection is disruptive, the population first converges to $z^* = \bar{q}$ (solid blue) or to either $z_1^* = \bar{q} - \theta$ or $z_2^* = \bar{q} + \theta$ (speckled blue). Dashed lines indicate the values used in *b* and *c*. *b*, *c*, Bifurcation diagrams for singular strategies as a function of E_{ST} (in *b* with $m = 0.65$) and dispersal m (in *c* with $E_{ST} = 0.4$). Other parameters are the same as in *a*. White circles indicate singular strategies that are evolutionary repellers; pink circles indicate singular strategies that are attractors and for which selection is stabilizing (solid: $z^* = \bar{q}$; crossed: $z_1^* = \bar{q} - \theta$ or $z_2^* = \bar{q} + \theta$); blue circles indicate singular strategies that are attractors and for which selection is disruptive (evolutionary branching points; solid: $z^* = \bar{q}$; crossed: $z_1^* = \bar{q} - \theta$ or $z_2^* = \bar{q} + \theta$). Dotted lines indicate the average resource property in each habitat, \bar{q}_1 and \bar{q}_2 . *d*, *f*, Phenotypic distribution in simulated populations after 2,000 years of evolution when the population becomes adapted to a single habitat (for $E_{ST} = 1$ in *d* and *e* and with populations initially monomorphic for $z = 49$ in *d* and $z = 51$ in *e*) or polymorphic (for $E_{ST} = 0.6$ in *f*). Other parameters: $n = 10$, $\gamma = 0$, $\sigma_r^2 = 2$, $\sigma_g^2 = 1$, and $m = 0.1$.

margin (fig. S1). In the limit of large patch size and weak dispersal, the leading term of χ_h reduces to that of χ_b . In contrast to condition (7), weaker resource differentiation E_{ST} always disfavors polymorphism in condition (9) (solid blue region in fig. 5a–5c). The reason is that here polymorphism is driven only by spatially disruptive selection. Variation of resources within patches weakens the strength of spatially disruptive selection because it allows individuals expressing the average resource trait \bar{q} to exploit some resources in both patch types.

Another contrasting result to the case with long exploitation time T is that the singular strategy $z^* = \bar{q}$ is no longer always an attractor of directional selection. Instead, for sufficiently large E_{ST} , $z^* = \bar{q}$ is an evolutionary repeller (speckled region in fig. 5a, 5b) as long as dispersal is not extremely limited (fig. 5c). When $z^* = \bar{q}$ is a repeller, the population trait value is attracted to either of two singular strategies: $z_1^* = \bar{q} - \theta$ (for some $\theta > 0$), which is closer to the average resource \bar{q}_1 within patches of type 1, or $z_2^* = \bar{q} + \theta$, which is closer to the average resource \bar{q}_2 within patches of type 2.

It is not possible to solve for z_1^* and z_2^* explicitly, but numerical explorations indicate that z_1^* and z_2^* approach \bar{q}_1 and \bar{q}_2 , respectively, when E_{ST} increases and m is intermediate (fig. 5b, 5c). Depending on initial conditions, the population thus either converges to become more adapted to patches of type 1 (if the population initially expresses a trait value $z < \bar{q}$) or to patches of type 2 (if the population initially expresses a trait value $z > \bar{q}$). This is due to the fact that patches where individuals are better locally adapted send out more offspring. As a result, if individuals are initially fitter in one habitat and migration is sufficiently high, offspring with traits more adapted to these patches swamp the population, which then evolves to become more adapted to this habitat.

Investigating numerically the nature of selection when the population expresses z_1^* or z_2^* reveals that for large patch differentiation E_{ST} , selection is stabilizing at these singular points (speckled pink region in fig. 5a–5c), so that the population is “stuck” being adapted to a single habitat (fig. 5d, 5e). When E_{ST} is intermediate, however, the population

experiences disruptive selection and thus becomes polymorphic (speckled blue region and crossed blue circles in fig. 5*a–5c*). Individual-based simulations confirm this and show that eventually the population again consists of two morphs, each more adapted to one habitat (fig. 5*f*). The end point of the dimorphic evolutionary dynamics does not depend on whether the population first converged to z_1^* or z_2^* . This shows that variation of resources within patches (so that $E_{ST} < 1$) allows the population to escape the evolutionary dead end of being adapted to only one habitat. Similarly, Meszena et al. (1997) found that intermediate patch divergence allowed the population to evolve polymorphism after first adapting to one patch type. Our model shows that these alternative routes to polymorphism can also be opened by variation of resources within patches.

Discussion

Our analyses indicate that polymorphism in a consumer trait emerges more readily when resources vary both within and between patches (when $\sigma_{r,w}^2 > 0$ and $\sigma_{r,b}^2 > 0$), in other words, when selection is simultaneously spatially and locally disruptive. Kin selection due to limited dispersal, by contrast, opposes polymorphism, especially when polymorphism is driven by locally disruptive selection. This is because local interactions among kin reduce the advantage of expressing alternative phenotypes to escape resource competition (Day 2001; Ajar 2003). Thus, although both spatially and locally disruptive selection contribute jointly to polymorphism, spatially disruptive selection is typically much stronger. One broad conclusion is therefore that polymorphism results more easily from local adaptation than from local competition, although both contribute to the evolution of phenotypic variation.

Our finding that spatially and locally disruptive selection act in concert in promoting polymorphism contrasts with a previous suggestion that they may oppose one another (i.e., that polymorphism emerges less easily when both forms of selection operate jointly; Day 2000). This suggestion was drawn from a two-patch model of resource competition excluding kin selection (effectively assuming that patches are of infinite sizes). While spatially and locally disruptive selection unfold from a microscopic ecological model in our study (in the spirit of Geritz and Kisdi 2004; our section “Resource Distribution and Consumption” and box 1), Day (2000) incorporates both types of selection independently by modifying equations of the Lotka-Volterra type in a way that Day (2000) himself refers to as “phenomenological” (p. 792). Locally disruptive selection is enforced by assuming that fecundity is limited by trait similarity with patch neighbors, and spatially disruptive selection is enforced by assuming that the carrying capacity of a patch decreases with the difference between a local phenotypic

optimum and the average trait expressed in that patch (eqq. [3], [4], and [8] in Day 2000). Under different models of population regulation, the growth rate at low density may depend on the resident trait (his eq. [22]) or not (his eq. [7]), which determines whether spatial heterogeneity either favors or hinders evolutionary branching. We are not aware of mechanistic derivations of Day’s equations and in fact find it difficult to conceive a microscopic ecological scenario where trait expression has independent effects on fecundity and carrying capacity. This makes explaining the biological basis for our diverging results difficult, at least to us. Nevertheless, the results in Day (2000) suggest that spatially and locally disruptive selection may not always work hand in hand toward polymorphism. To disentangle potential effects stemming from varying carrying capacity, it would be interesting to extend our approach to consider scenarios where local demography changes endogenously with trait evolution (Rousset and Ronce 2004).

Whether selection leads to polymorphism is a different question from how selection shapes variation within and between patches once polymorphism has emerged. To this question, spatially and locally disruptive selection offer opposite answers: spatially disruptive selection favors local adaptation and phenotypic differentiation between patches, while locally disruptive selection favors variation within patches. Presumably, these antagonistic effects do not depend on the ecological scenario that leads to locally disruptive selection (which in our model is due to trait-dependent resource competition within patches). For instance, Bolnick and Stutz (2017) analyze a two-patch population genetics model with a locus subject to (i) negative frequency-dependent selection within patches, in which the rarer allele in a patch is locally favored to capture an ecological situation where parasites evolve to target the most abundant local type, and (ii) selection for local adaptation, so that each allele is associated with greater fitness in a specific patch. Similarly to us, Bolnick and Stutz (2017) find that by increasing effective gene flow, negative frequency-dependent selection reduces allelic divergence among patches.

To quantify divergence among patches, we apply the popular Q_{ST} measure of trait differentiation. This measure has been widely used in comparison to neutral genetic differentiation F_{ST} to infer the nature of selection in empirical studies (Leinonen et al. 2013). The commonly accepted interpretation of Q_{ST}/F_{ST} comparisons is that (1) $Q_{ST} > F_{ST}$ indicates spatially disruptive selection (i.e., local adaptation), (2) $Q_{ST} = F_{ST}$ indicates neutral evolution, and (3) $Q_{ST} < F_{ST}$ indicates spatially uniform selection (i.e., stabilizing selection for the same trait value in all patches; e.g., Whitlock 2008; Leinonen et al. 2013). In contrast, our results show that spatially uniform selection leads to $Q_{ST} = F_{ST}$. In line with this result, a simulation study by

Whitlock and Guillaume (2009) finds that spatially uniform selection leads at best to a weak signal of $Q_{ST} < F_{ST}$ (when the phenotypic effects of mutations are large relative to selection), so that statistical methods have low detection power (their fig. 6 especially). Nevertheless, signals of $Q_{ST} < F_{ST}$ have been detected in several natural populations for a wide range of traits (e.g., Merilä and Crnokrak 2001; McKay and Latta 2002; Leinonen et al. 2008; Marin et al. 2020) and have been interpreted as evidence of spatially uniform selection. Based on our results, an alternative suggestion is that $Q_{ST} < F_{ST}$ results from traits being under locally disruptive selection, which causes greater divergence within patches than expected under random gene flow (as verbally argued in Lamy 2012). In snapdragon plants, for example, germination date shows lower levels of Q_{ST} relative to F_{ST} (Marin et al. 2020). Since germination date can mediate competition for resources (Elzinga et al. 2007), such a pattern may in fact be due to locally disruptive selection. It would

therefore be relevant to study more formally the statistical power of Q_{ST}/F_{ST} comparisons when frequency dependence promotes local polymorphism and thereby contributes to $Q_{ST} < F_{ST}$.

Our simulations focus on situations where two morphs eventually coexist in the population, but there are cases in which more than two morphs may emerge and be maintained (fig. 6a; Geritz et al. 1998). In the context of our model, multiple morphs may evolve when there are multiple patch types (i.e., the distribution in the top of fig. 1d is multi peaked), so that spatially disruptive selection favors local adaptation to many different habitats, or when the degree of generalism σ_g^2 is much smaller than within-patch resource variation σ_r^2 , leading to strong locally disruptive selection to avoid within-patch competition for resources. In principle, spatially disruptive selection favors as many morphs as there are habitats, and locally disruptive selection favors as many morphs as there are local niches. But

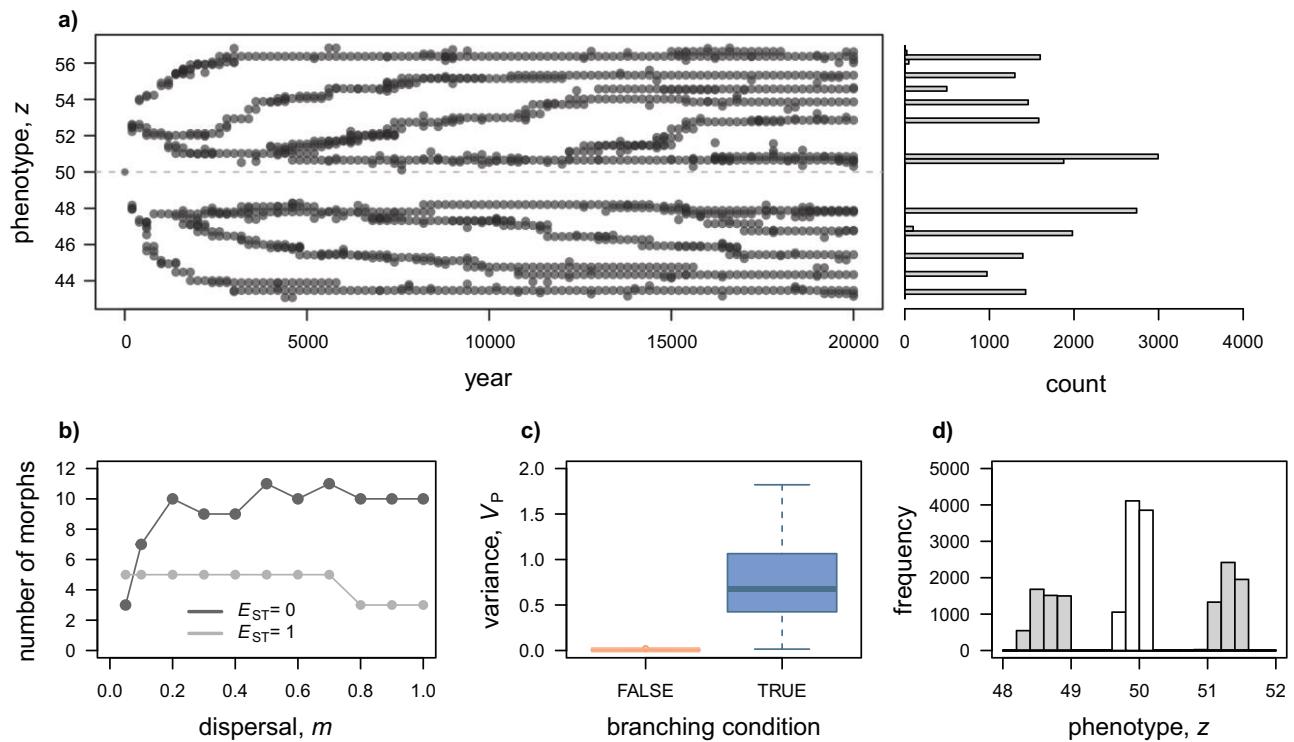


Figure 6: Emergence of multiple morphs and evolution under sexual reproduction. *a*, Simulated evolution of the consumer trait z when the resource distribution is wide relative to the degree of generalism, leading to the emergence of multiple morphs ($\sigma_r^2 = 25$, $\sigma_g^2 = 1$). Other parameters: $E_{ST} = 0$, $\gamma = 0$, $n = 10$, and $m = 0.5$. *b*, Number of morphs after 20,000 years of simulated evolution as a function of dispersal for $E_{ST} = 0$ (in black) and $E_{ST} = 1$ (in gray). Other parameters: $\sigma_r^2 = 5$ with five habitat types, $\sigma_g^2 = 1$, $\gamma = 0$, and $n = 10$. This shows that the number of morphs increase with dispersal when selection is locally and decreases when selection is spatially disruptive. *c*, Boxplots for the distribution of phenotypic variance V_P across 66 simulations with different parameters under sexual reproduction according to whether the branching condition (7) is met (49 simulations, in blue) or not (17 simulations, in pink). The 66 simulations correspond to all combinations of the following parameter values: $\sigma_r^2 = 1, 2$; $E_{ST} = 0, 0.5, 1$; $m = 0.05, 0.1, 0.2, \dots, 1.0$. Fixed parameters: $\sigma_g^2 = 1$, $n = 10$, and $\gamma = 0$. Phenotypic variances are measured after 2,000 years of evolution during step 4 of the annual life cycle. *d*, Phenotypic distribution in a simulated population of sexually reproducing individuals after 2,000 years of evolution. Parameters: $\sigma_g^2 = 1$, $n = 10$, $\gamma = 0$, $\sigma_r^2 = 2$, $E_{ST} = 0.5$, and $m = 0.5$. The most-diverged phenotypes are shown in gray, while hybrids are shown in white.

whether that many morphs actually evolve should depend on the degree of gene flow, with presumably fewer morphs under locally disruptive selection and more under spatially disruptive selection when dispersal is limited. Individual-based simulations confirm this, with the number of morphs increasing with dispersal when $E_{ST} = 0$ (black line in fig. 6*b*) and decreasing when $E_{ST} = 1$ (gray line in fig. 6*b*). To study this more definitively it would be necessary, although challenging, to perform an analysis in subdivided polymorphic populations with finite patch size.

Our model assumes clonal reproduction, but previous theory suggests that our condition (7) for evolutionary branching and the emergence of differentiated morphs should equally hold under sexual reproduction (Kisdi and Geritz 1999). To test this, we performed additional simulations where diploid individuals mate randomly within patches and the trait is determined by additive effects at one locus (for details, see sec. S4 of the supplemental PDF). These simulations show that trait variation is significantly greater when condition (7) is satisfied than when it is not (fig. 6*c*). In contrast to the case of clonal reproduction, the trait distribution in the population shows three instead of two morphs, as mating among diverged genotypes creates intermediate hybrids (fig. 6*d*). As these hybrids are less fit, selection should in turn favor mechanisms such as allelic dominance (Van Dooren 1999) or assortative mating (Geritz and Kisdi 2000) to prevent the formation of intermediate phenotypes (Slatkin 1984; for other mechanisms, see Kopp and Hermisson 2006; van Doorn and Dieckmann 2006; for a review, see Rueffler et al. 2006*a*). It would be interesting to extend our model to investigate the evolution of genetic and behavioral mechanisms that can avoid the production of unfit hybrids, especially because spatially and locally disruptive selection may favor the evolution of different mechanisms depending on dispersal and gene flow, with potential implications for speciation.

To conclude, our study helps us understand the conditions under which resource variation within and between habitats leads to adaptive polymorphism in consumer traits as well as how this polymorphism is distributed in the population. More broadly, by combining three fundamental sources of selection in spatially structured populations—exploitation competition, local adaptation, and interactions among kin—our model takes a step further toward integrating different strands of the theory of adaptation.

Acknowledgments

We thank Erol Akçay, Michael Kopp, and an anonymous reviewer for helpful comments on the manuscript. C.M. is funded by Swiss National Science Foundation grant PCEFP3181243.

Statement of Authorship

M.S., C.R., L.L., and C.M. conceived the model and study. M.S. and C.M. performed the analyses with contributions from C.R. and L.L. The first draft of the manuscript was written by M.S. and C.M. All authors contributed to the final version.

Data and Code Availability

Data and code are available on Figshare (<https://doi.org/10.6084/m9.figshare.23617305>; Schmid et al., 2023).

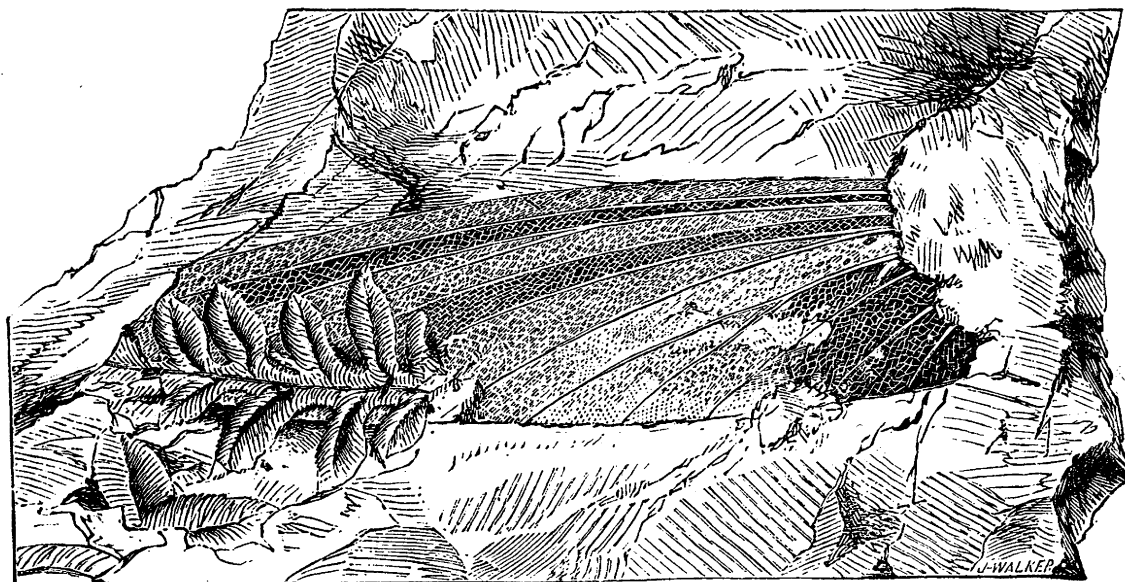
References

- Abrams, P. A. 1986. Character displacement and niche shift analyzed using consumer-resource models of competition. *Theoretical Population Biology* 29:107–160.
- Abrams, P. A., C. Rueffler, and G. Kim. 2008. Determinants of the strength of disruptive and/or divergent selection arising from resource competition. *Evolution* 62:1571–1586.
- Ajar, E. 2003. Analysis of disruptive selection in subdivided populations. *BMC Evolutionary Biology* 3:22.
- Berner, D., M. Roesti, A. P. Hendry, and W. Salzburger. 2010. Constraints on speciation suggested by comparing lake-stream stickleback divergence across two continents. *Molecular Ecology* 19:4963–4978.
- Bolnick, D. I., and W. E. Stutz. 2017. Frequency dependence limits divergent evolution by favouring rare immigrants over residents. *Nature* 546:285–288.
- Boussange, V., and L. Pellissier. 2022. Eco-evolutionary model on spatial graphs reveals how habitat structure affects phenotypic differentiation. *Communications Biology* 5:668.
- Brown, J. S., and N. B. Pavlovic. 1992. Evolution in heterogeneous environments: effects of migration on habitat specialization. *Evolutionary Ecology* 6:360–382.
- Christiansen, F. B. 1975. Hard and soft selection in a subdivided population. *American Naturalist* 109:11–16.
- Christiansen, F. B., and V. Loeschcke. 1980. Evolution and intraspecific exploitative competition. I. One-locus theory for small additive gene effects. *Theoretical Population Biology* 18:297–313.
- Cotto, O., M. Schmid, and F. Guillaume. 2020. Nemo-age: spatially explicit simulations of eco-evolutionary dynamics in stage-structured populations under changing environments. *Methods in Ecology and Evolution* 11:1227–1236.
- Day, T. 2000. Competition and the effect of spatial resource heterogeneity on evolutionary diversification. *American Naturalist* 155:790–803.
- . 2001. Population structure inhibits evolutionary diversification under competition for resources. *Genetica* 112/113:71–86.
- Débarre, F., and S. Gandon. 2011. Evolution in heterogeneous environments: between soft and hard selection. *American Naturalist* 177:E84–E97.
- Dieckmann, U., and M. Doebeli. 1999. On the origin of species by sympatric speciation. *Nature* 400:354–357.
- Elzinga, J. A., A. Atlan, A. Biere, L. Gigord, A. E. Weis, and G. Bernasconi. 2007. Time after time: flowering phenology and

- biotic interactions. *Trends in Ecology and Evolution* 22:432–439.
- Felsenstein, J. 1976. Theoretical population-genetics of variable selection and migration. *Annual Review of Genetics* 10:253–280.
- Frank, S. A. 1998. *Foundations of social evolution*. Princeton University Press, Princeton, NJ.
- Geritz, S. A. H., and E. Kisdi. 2000. Adaptive dynamics in diploid, sexual populations and the evolution of reproductive isolation. *Proceedings of the Royal Society B* 267:1671–1678.
- . 2004. On the mechanistic underpinning of discrete-time population models with complex dynamics. *Journal of Theoretical Biology* 228:261–269.
- Geritz, S. A. H., E. Kisdi, G. Meszéna, and J. A. J. Metz. 1998. Evolutionary singular strategies and the adaptive growth and branching of the evolutionary tree. *Evolutionary Ecology* 12:35–57.
- Grant, B. R., and P. R. Grant. 2008. Fission and fusion of Darwin's finches populations. *Philosophical Transactions of the Royal Society B* 363:2821–2829.
- Grant, P. R., and B. R. Grant. 2002. Unpredictable evolution in a 30-year study of Darwin's finches. *Science* 296:707–711.
- Haldane, J. B. 1948. The theory of a cline. *Journal of Genetics* 48:277–284.
- Hamilton, W. D. 1964. The genetical evolution of social behaviour, I and II. *Journal of Theoretical Biology* 7:1–52.
- Hendry, A. P., E. B. Taylor, and J. D. McPhail. 2002. Adaptive divergence and the balance between selection and gene flow: lake and stream stickleback in the Misty system. *Evolution* 56:1199–1216.
- Hereford, J. 2009. A quantitative survey of local adaptation and fitness trade-offs. *American Naturalist* 173:579–588.
- Hirshleifer, J. 1989. Conflict and rent-seeking success functions: ratio vs. difference models of relative success. *Public Choice* 63:101–112.
- Kawecki, T. J., and D. Ebert. 2004. Conceptual issues in local adaptation. *Ecology Letters* 7:1225–1241.
- Kisdi, E., and S. A. H. Geritz. 1999. Adaptive dynamics in allele space: evolution of genetic polymorphism by small mutations in a heterogeneous environment. *Evolution* 53:993–1008.
- Kopp, M., and J. Hermisson. 2006. The evolution of genetic architecture under frequency-dependent disruptive selection. *Evolution* 60:1537–1550.
- Lamy, J. B., C. Plomion, A. Kremer, and S. Delzon. 2012. $Q_{ST} < F_{ST}$ as a signature of canalization. *Molecular Ecology* 21:5646–5655.
- Leimu, R., and M. Fischer. 2008. A meta-analysis of local adaptation in plants. *PLoS ONE* 3:e4010.
- Leinonen, T., R. J. S. McCairns, R. B. O'Hara, and J. Merilä. 2013. $Q_{ST} - F_{ST}$ comparisons: evolutionary and ecological insights from genomic heterogeneity. *Nature Reviews Genetics* 14:179–190.
- Leinonen, T., R. B. O'Hara, J. M. Cano, and J. Merilä. 2008. Comparative studies of quantitative trait and neutral marker divergence: a meta-analysis. *Journal of Evolutionary Biology* 21:1–17.
- Lenormand, T. 2002. Gene flow and the limits to natural selection. *Trends in Ecology and Evolution* 17:183–189.
- Levene, H. 1953. Genetic equilibrium when more than one ecological niche is available. *American Naturalist* 87:331–333.
- MacArthur, R. H., and R. Levins. 1967. The limiting similarity, convergence, and divergence of coexisting species. *American Naturalist* 101:377–385.
- Marin, S., A. Gibert, J. Archambeau, V. Bonhomme, M. Lascoste, and B. Pujol. 2020. Potential adaptive divergence between sub-species and populations of snapdragon plants inferred from $Q_{ST} - F_{ST}$ comparisons. *Molecular Ecology* 29:3010–3021.
- Maynard Smith, J. 1962. Disruptive selection, polymorphism and sympatric speciation. *Nature* 195:60–62.
- McDonald, T. K., and S. Yeaman. 2018. Effect of migration and environmental heterogeneity on the maintenance of quantitative genetic variation: a simulation study. *Journal of Evolutionary Biology* 31:1386–1399.
- McKay, J. K., and R. G. Latta. 2002. Adaptive population divergence: markers, QTL and traits. *Trends in Ecology and Evolution* 17:285–291.
- Merilä, J., and P. Crnokrak. 2001. Comparison of genetic differentiation at marker loci and quantitative traits. *Journal of Evolutionary Biology* 14:892–903.
- Meszéna, G., I. Czibula, and S. A. H. Geritz. 1997. Adaptive dynamics in a 2-patch environment: a toy model for allopatric and parapatric speciation. *Journal of Biological Systems* 5:265–284.
- Michod, R. E. 1982. The theory of kin selection. *Annual Review of Ecology and Systematics* 13:23–55.
- Mullon, C., and L. Lehmann. 2019. An evolutionary quantitative genetics model for phenotypic (co)variances under limited dispersal, with an application to socially synergistic traits. *Evolution* 73:1695–1728.
- Ohtsuki, H., C. Rueffler, J. Y. Wakano, K. Parvinen, and L. Lehmann. 2020. The components of directional and disruptive selection in heterogeneous group-structured populations. *Journal of Theoretical Biology* 507:110449.
- Ovaskainen, O., M. Karhunen, C. Zheng, J. M. C. Arias, and J. Merilä. 2011. A new method to uncover signatures of divergent and stabilizing selection in quantitative traits. *Genetics* 189:621–632.
- Ravinet, M., P. A. Prodöhl, and C. Harrod. 2013. Parallel and non-parallel ecological, morphological and genetic divergence in lake-stream stickleback from a single catchment. *Journal of Evolutionary Biology* 26:186–204.
- Rettelbach, A., M. Kopp, U. Dieckmann, and J. Hermisson. 2013. Three modes of adaptive speciation in spatially structured populations. *American Naturalist* 182:E215–E234.
- Ronce, O., and M. Kirkpatrick. 2001. When sources become sinks: migrational meltdown in heterogeneous habitats. *Evolution* 55:1520–1531.
- Rosenzweig, M. L. 1978. Competitive speciation. *Biological Journal of the Linnean Society* 10:275–289.
- Roughgarden, J. 1976. Resource partitioning among competing species—a coevolutionary approach. *Theoretical Population Biology* 9:388–424.
- Rousset, F. 2004. *Genetic structure and selection in subdivided populations*. Princeton University Press, Princeton, NJ.
- Rousset, F., and O. Ronce. 2004. Inclusive fitness for traits affecting metapopulation demography. *Theoretical Population Biology* 65:127–141.
- Rueffler, C., T. J. M. Van Dooren, O. Leimar, and P. A. Abrams. 2006a. Disruptive selection and then what? *Trends in Ecology and Evolution* 21:238–245.
- Rueffler, C., T. J. M. Van Dooren, and J. A. J. Metz. 2006b. The evolution of resource specialization through frequency-dependent and frequency-independent mechanisms. *American Naturalist* 167:81–93.
- Schmid, M., C. Rueffler, L. Lehmann, and C. Mullon. 2023. Data from: Resource variation within and between patches: Where

- exploitation competition, local adaptation, and kin selection meet. *American Naturalist*, Figshare, <https://doi.org/10.6084/m9.figshare.23617305>.
- Skúlason, S., and T. B. Smith. 1995. Resource polymorphisms in vertebrates. *Trends in Ecology and Evolution* 10:366–370.
- Slatkin, M. 1979. Frequency- and density-dependent selection on a quantitative character. *Genetics* 93:755–771.
- . 1980. Ecological character displacement. *Ecology* 61:163–177.
- . 1984. Ecological causes of sexual dimorphism. *Evolution* 38:622–630.
- Smith, T. B., and S. Skúlason. 1996. Evolutionary significance of resource polymorphisms in fishes, amphibians, and birds. *Annual Review of Ecology and Systematics* 27:111–133.
- Svardal, H., C. Rueffler, and J. Hermisson. 2015. A general condition for adaptive genetic polymorphism in temporally and spatially heterogeneous environments. *Theoretical Population Biology* 99:76–97.
- Taylor, P. D. 1992. Altruism in viscous populations—an inclusive fitness model. *Evolutionary Ecology* 6:352–356.
- Van Dooren, T. J. M. 1999. The evolutionary ecology of dominance-recessivity. *Journal of Theoretical Biology* 198:519–532.
- van Doorn, G. S., and U. Dieckmann. 2006. The long-term evolution of multilocus traits under frequency-dependent disruptive selection. *Evolution* 60:2226–2238.
- Wallace, B. 1975. Hard and soft selection revisited. *Evolution* 29:465–473.
- Weir, B. S., and C. C. Cockerham. 1984. Estimating F -statistics for the analysis of population structure. *Evolution* 38:1358–1370.
- Whitlock, M. C. 2008. Evolutionary inference from Q_{ST} . *Molecular Ecology* 17:1885–1896.
- Whitlock, M. C., and F. Guillaume. 2009. Testing for spatially divergent selection: comparing Q_{ST} to F_{ST} . *Genetics* 183:1055–1063.

Associate Editor: Michael Kopp
 Editor: Erol Akçay



“*Haplophlebia Barnesii*. A curious neuropterous insect, of large size, probably allied to our May-flies; taken by Mr. Barnes from the coal of Cape Breton.” From “The Insects of Ancient America” by S. H. Scudder (*The American Naturalist*, 1868, 1:625–631).

Supplementary Material to "Resource variation within and between patches: Where exploitation competition, local adaptation and kin selection meet"

Max Schmid^{1,2}, Claus Rueffler³, Laurent Lehmann¹ and Charles Mullan^{1,*}

¹Department of Ecology and Evolution, University of Lausanne, 1015 Lausanne, Switzerland

²Department of Biology, University of Tübingen, 72076 Tübingen, Germany

³Department of Ecology and Genetics, Animal Ecology, Uppsala University, 75236 Uppsala, Sweden

*Correspondence: charles.mullan@unil.ch

S1 Fitness

Here, we specify individual fitness, which is the basis of our evolutionary analysis.

S1.1 Individual fitness

From individual fecundity (eq. 5 with eq. I.C in Box I), we can determine individual fitness, which is here defined as the expected number of successful offspring an individual produces over one full iteration of the life cycle (including itself if it survives). For our analysis specifically (which is based on Ohtsuki et al., 2020, see Appendix S2 below), we need to characterize the fitness function $w_{s'|s}(z_1, \mathbf{z}_{-1}, z)$, which gives the expected number of offspring that settle in patches of state s' and that descend from an individual with trait z_1 in a patch in state s , where the patch neighbors of the focal individual express traits $\mathbf{z}_{-1} = (z_2, z_3, \dots, z_n)$ and the rest of the population is monomorphic for z (i.e., we only consider variation in the focal patch).

S1.1.1 Decomposing fitness

Following Ohtsuki et al. (2020), we first decompose individual fitness into two components,

$$w_{s'|s}(z_1, \mathbf{z}_{-1}, z) = \begin{cases} w_{s|s}^p(z_1, \mathbf{z}_{-1}, z) + w_{s|s}^d(z_1, \mathbf{z}_{-1}, z), & \text{for } s' = s, \\ w_{s'|s}^d(z_1, \mathbf{z}_{-1}, z), & \text{for } s' \neq s, \end{cases} \quad (\text{S1})$$

where $w_{s'|s}^d(z_1, \mathbf{z}_{-1}, z)$ is the expected number of offspring that settles in non-natal patches of state s' , which we refer to as the dispersal component of fitness, and $w_{s|s}^p(z_1, \mathbf{z}_{-1}, z)$ is the expected number of non-dispersing descendants (including the focal individual if it survives), which we refer to as the philopatric component. This component can be further decomposed into survival and reproduction components as

$$w_{s|s}^p(z_1, \mathbf{z}_{-1}, z) = \gamma + n(1 - \gamma)\phi_{s|s}^p(z_1, \mathbf{z}_{-1}, z), \quad (\text{S2})$$

where γ is the probability of survival, and $\phi_{s|s}^p(z_1, \mathbf{z}_{-1}, z)$ is the probability that an open breeding spot (of which there are $n(1 - \gamma)$ on average before the regulation stage) is filled by a philopatric offspring of the focal individual (with $n\phi_{s|s}^p(z_1, \mathbf{z}_{-1}, z)$ corresponding to $w_{1,s|s}^{pr}$ in Ohtsuki et al., 2020). Similarly, we write the dispersal component of fitness as

$$w_{s'|s}^d(z_1, \mathbf{z}_{-1}, z) = n(1 - \gamma)\phi_{s'|s}^d(z_1, \mathbf{z}_{-1}, z) \quad (\text{S3})$$

where $\phi_{s'|s}^d(z_1, \mathbf{z}_{-1}, z)$ is the probability that a dispersing offspring of the focal individual settles in an empty breeding spot in a patch of type s' (note that $n\phi_{s'|s}^d(z_1, \mathbf{z}_{-1}, z)$ corresponds to $w_{1,s'|s}^{pr}$ in Ohtsuki et al., 2020).

The probability that an offspring of the focal individual (with trait z_1) fills a spot in the focal patch is given by

$$\phi_{s|s}^p(z_1, \mathbf{z}_{-1}, z) = \frac{(1 - m)f_s(z_1, \mathbf{z}_{-1})}{(1 - m)\sum_{i=1}^n f_s(z_i, \mathbf{z}_{-i}) + nmf(z)}, \quad (\text{S4})$$

where

$$f(z) = \sum_{s \in \Omega} \pi_s f_s(z), \quad (\text{S5})$$

is the average fecundity in a monomorphic population, which depends on

$$f_s(z) = \frac{k}{n} \sum_{j=1}^{n_R} \beta R_{j,s}(0) (1 - e^{-Tn\alpha(z, q_j)}), \quad (\text{S6})$$

the fecundity of an individual in a patch in state s when all individuals in the patch express the same trait, z (i.e., under neutrality), which is obtained from eqs. (5) and (I.C) and setting $z_1 = z_2 = \dots = z_n = z$. Eq. (S4) thus consists of the ratio of the number of offspring of the focal individual that remain in their natal patch to the total number of offspring that enter competition, which is decomposed into the sum of those that are philopatric and those that come from other patches (which we recall here are assumed to be monomorphic for the resident z). Similarly, the probability that a dispersing offspring of the focal individual fills a spot in a patch

in state s' can be expressed as

$$\phi_{s'|s}^d(z_1, \mathbf{z}_{-1}, z) = \pi_{s'} \frac{m f_s(z_1, \mathbf{z}_{-1})}{n(1-m) f_{s'}(z) + n m f(z)}, \quad (\text{S7})$$

where the numerator corresponds to the total number of offspring of the focal individual that disperse into patches in state s' , and the denominator to the total number of offspring that compete for a spot in such a patch.

S1.1.2 Fitness components in a monomorphic population

As they will be relevant to our analysis, we also give here the components of fitness when the population is monomorphic for z . In this case, we obtain from eqs. (S4)-(S7) that

$$\phi_{s'|s}^p(z) = \frac{(1-m) f_s(z)}{(1-m) n f_s(z) + n m f(z)} \quad (\text{S8})$$

for the philopatric component, and

$$\phi_{s'|s}^d(z) = \pi_{s'} \frac{m f_s(z)}{(1-m) n f_{s'}(z) + n m f(z)} \quad (\text{S9})$$

for the dispersal component.

S2 Method

S2.1 Evolution on two time scales

In this Appendix, we describe the approach we take to model the evolution of the consumer trait z , assuming mutations are constantly occurring at a small rate and have small phenotypic effects. Under these assumptions, trait evolution can be decomposed into two timescales (Metz et al., 1996; Geritz et al., 1998; Dercole and Rinaldi, 2008). First, the trait evolves under directional selection, gradually evolving larger or smaller trait values under the influx of mutations. The population may thus attain a "convergence stable strategy", which is an attractor of directional evolution. Second, selection is either stabilizing, in which case the population remains unimodally distributed around the convergence stable strategy, or disruptive, in which case the trait becomes polymorphic and differentiated with individuals expressing either large or small trait values.

Our approach to understand directional and stabilizing/disruptive selection is based on an evolutionary invasion analysis for populations that are divided into an infinite number of non-homogeneous groups (Ohtsuki et al., 2020). This analysis looks at the evolutionary success of a single copy of a mutant allele coding for a mutant trait value that is introduced in an otherwise monomorphic population with a resident trait value, applying

the theory of multi-type branching processes (Appendix A.1 of Ohtsuki et al., 2020 for details). Whether the mutant goes extinct or spreads in the population is determined by the mutant's invasion fitness, from which the selection gradient and coefficient of disruptive selections reported below are derived. Invasion fitness is calculated when the mutant is rare in the population, i.e., the size of the mutant lineage is finite in an otherwise infinite population, so that individuals from the mutant lineage do not interact with one another when in different patches. But owing to limited dispersal and finite patch size, individuals from the mutant lineage do interact with one another within patches where mutants reside, which leads to kin selection. We summarize the approach below with a focus on our model (see Ohtsuki et al., 2020 for more general problems, e.g., where the sizes of patches varies).

S2.2 Directional selection

S2.2.1 Selection gradient

The selection gradient, $S(z)$, tells us whether selection favors an increase (when $S(z) > 0$) or decrease (when $S(z) < 0$) in the trait when the population is monomorphic for z . Accordingly, a (locally) convergence stable strategy z^* is such that

$$S(z^*) = 0, \quad (\text{S10})$$

i.e., it is a "singular strategy" where directional selection vanishes, and

$$\left. \frac{dS(z)}{dz} \right|_{z=z^*} < 0, \quad (\text{S11})$$

i.e., a population away from this singular strategy is attracted to it.

S2.2.2 Selection gradient in patch-structured populations

It has been shown for populations divided into heterogeneous patches that the selection gradient can be expressed in terms of individual fitness as,

$$S(z) = \sum_{s' \in \Omega} \sum_{s \in \Omega} v_{s'}(z) \left[\frac{\partial w_{s'|s,1}}{\partial z_1} + (n-1)r_{2,s}(z) \frac{\partial w_{s'|s,1}}{\partial z_2} \right] p_s(z) \quad (\text{S12})$$

(e.g., eq. E.17 in Lehmann et al., 2016, eq. 32 in Ohtsuki et al., 2020), where we have used the short-hand notation

$$w_{s'|s,1} = w_{s'|s}(z_1, \mathbf{z}_{-1}, z) \quad (\text{S13})$$

to denote the fitness of a focal individual, and here and hereafter all derivatives are evaluated in a monomorphic resident population at z (i.e., where $z_i = z$ for all i). In eq. (S12), $p_s(z)$ is the probability that a randomly sampled individual from a resident lineage (i.e., whose members express z) resides in a patch in state s (the frequency

distribution among patch states in a resident population), which can be thought of as the contexts in which a mutation changing trait value can arise. The term within square brackets is the sum of the direct ($\partial w_{s'|s,1}/\partial z_1$) and relatedness-weighted indirect ($\partial w_{s'|s,1}/\partial z_2$) effects of varying trait expression on the expected number of offspring that an individual in a patch in state s leaves in patches in state s' , where $r_{2,s}(z)$ is the probability that two randomly sampled individuals from a patch in state s are identical-by-descent (pairwise relatedness) under neutrality. Hence, this term in square brackets can be thought of as the net effect on the expected number of offspring that settle in a patch in state s' descending from a parent in a patch in state s , due to a change in the trait of all the members of the lineage of this parent. Finally, each offspring needs to be weighted by its reproductive value $v_{s'}(z)$, which is its asymptotic contribution to the future of the population in patches of state s' in the absence of selection (and thus takes into account the demographic consequences of such offspring). The three quantities $p_s(z)$, $r_{2,s}(z)$, $v_{s'}(z)$ are evaluated under the assumption that the population is monomorphic for z . For a detailed derivation of eq. (S12), see Lehmann et al. (2016) and Ohtsuki et al. (2020) (note that, so far, our equations apply to both soft and hard selection).

Relatedness can be derived using standard identity-by arguments (e.g. Karlin, 1968; Rousset, 2004). For our model, such an argument leads to a recursion which at equilibrium satisfies

$$r_{2,s}(z) = \gamma^2 r_{2,s}(z) + 2\gamma(1-\gamma)(1-d_s(z))r_{2,s}^R(z) + (1-\gamma)^2(1-d_s(z))^2 r_{2,s}^R(z), \quad (\text{S14})$$

where

$$r_{2,s}^R(z) = \frac{1}{n} + \frac{n-1}{n} r_{2,s}(z), \quad (\text{S15})$$

is the probability that two individuals sampled with replacement (hence the superscript R) from a patch in state s are identical-by-descent, and

$$d_s(z) = \frac{mf(z)}{(1-m)f_s(z) + mf(z)} \quad (\text{S16})$$

is the backward probability of dispersal, i.e., the probability that an individual sampled in a patch of type s is an immigrant in a population monomorphic for z . Solving eq. (S14) for $r_{2,s}(z)$ then gives

$$r_{2,s}(z) = \frac{2\gamma(1-d_s(z)) + (1-\gamma)(1-d_s(z))^2}{n(1+\gamma) - 2\gamma(n-1)(1-d_s(z)) - (1-\gamma)(n-1)(1-d_s(z))^2}, \quad (\text{S17})$$

which agrees with eqs. (52) of Ohtsuki et al. (2020) that was derived with a different method. Meanwhile, the product between the parental state distribution $p_s(z)$ and the offspring reproductive value $v_{s'}(z)$ appearing in eq. (S12) is given by,

$$v_{s'}(z)p_s(z) = \frac{\phi_{s|s'}^d(z)}{(1-\gamma)\left(1 - n\phi_{s'|s'}^p(z)\right)\left(1 - n\phi_{s|s}^p(z)\right)} \bigg/ \left(\sum_{s'' \in \Omega} \frac{\phi_{s''|s''}^d(z)}{(1-\gamma)\left(1 - n\phi_{s''|s''}^p(z)\right)^2} \right) \quad (\text{S18})$$

(from eq. 40 in Ohtsuki et al., 2020).

S2.2.3 Selection gradient with fecundity effects

Substituting for individual fitness $w_{s'|s}(z_1, z_{-1}, z)$ in eq. (S12) with the explicit expression derived in Appendix A for our model (eqs. S1-S9; see also eq. I10 and eq. H10 in Ohtsuki et al., 2020 for more general results), we find after some re-arrangements that the selection gradient reduces to a single sum over patch states that can be written as

$$S(z) = \sum_{s \in \Omega} (1 - \gamma) \left[F_s(z) - \Phi_s(z)^2 r_{2,s}^R(z) \bar{F}_s(z) \right] v_s(z) p_s(z), \quad (\text{S19})$$

where $v_s(z) p_s(z)$ is the reproductive value of class s , i.e., the probability that an individual randomly sampled from the population descends from an individual reproducing in a patch in state s (satisfying $\sum_{s \in \Omega} v_s(z) p_s(z) = 1$, e.g., Taylor, 1990; Rousset, 2004). Selection in patches of type s then depends on the fraction of open breeding spots $(1 - \gamma)$ and on

$$F_s(z) = \frac{\partial f_{s,1}}{\partial z_1} + (n - 1) r_{2,s}^R(z) \frac{\partial f_{s,1}}{\partial z_2}, \quad (\text{S20})$$

where we used

$$f_{s,1} = \frac{f_s(z_1, z_{-1})}{f_s(z)}, \quad (\text{S21})$$

for the fecundity of a focal individual relative to fecundity in a population monomorphic for z (we drop the dependencies on phenotypes for the sake of brevity). Accordingly, $F_s(z)$ is the sum of the direct and relatedness-weighted fecundity effects of the trait in patches of type s relative to $f_s(z)$. This indicates that selection tends to favor trait values that increase the fecundity of an individual and of its relatives.

But when a trait increases the fecundity of its bearer and/or of its relatives, this also leads to an increase in kin competition within patches which in turn tends to reduce the strength of selection. Such effect is captured in eq. (S19) by $\Phi_s(z)^2 r_{2,s}^R(z) \bar{F}_s(z)$ which consists of three terms. The first, $\Phi_s(z)^2$ gives the probability that two offspring born in the same patch of type s compete with one another in a population monomorphic for z , since

$$\Phi_s(z) = 1 - d_s(z) \quad (\text{S22})$$

is the probability that a randomly sampled individual in a patch in state s is philopatric. Kin competition also increases with the probability $r_{2,s}^R(z)$ that two offspring sampled before dispersal in a patch of type s are identical-by-descent (given in eq. S15), and

$$\bar{F}_s(z) = \frac{\partial f_{s,1}}{\partial z_1} + (n - 1) \frac{\partial f_{s,1}}{\partial z_2}, \quad (\text{S23})$$

which is the total effect of the trait on relative fecundity, i.e., the effect on the fecundity of a focal individual in a patch of type s if every individual in the patch increase their trait value infinitesimally. Altogether, eq. (S19) thus reflects the balance between the positive effects of a trait change when such a change increases fecundity and its negative indirect effects through increased kin competition.

It is useful to note that the class reproductive value can be written as

$$v_s(z) p_s(z) = K_s(z) \pi_s \quad (\text{S24})$$

where

$$K_s(z) = \frac{f_s(z)}{f(z)} \frac{\frac{f_s(z)}{f(z)}(1-m) + m}{C_{v,f}^2(z)(1-m) + 1} \quad (\text{S25})$$

in which

$$C_{v,f}(z) = \sqrt{\sum_{s \in \Omega} \pi_s \left(\frac{f_s(z)}{f(z)} - 1 \right)^2} \quad (\text{S26})$$

is the coefficient of variation in fecundity among patch states, i.e., the ratio of the standard deviation to the mean fecundity. Hence, in the absence of fecundity variation across patches, $K_s(z) = 1$ for all $s \in \Omega$.

S2.3 Disruptive versus stabilizing selection

S2.3.1 Disruptive selection coefficient

Once the population has converged to a singular strategy z^* (so that it satisfies eqs. S10-S11), whether selection is stabilizing or disruptive depends on the sign of the coefficient of disruptive selection, which we denote generically as $H(z)$. Specifically, selection is stabilizing and the population remains monomorphic for the convergence stable strategy z^* when $H(z^*) < 0$, and conversely selection is disruptive leading to polymorphism when $H(z^*) > 0$ (Geritz et al., 1998; Dercole and Rinaldi, 2008; Rousset, 2004).

S2.3.2 Disruptive selection coefficient in patch-structured populations

In a non-homogeneous group-structured population, the coefficient of disruptive selection has been shown to be composed of three biologically relevant terms,

$$H(z) = H_w(z) + H_p(z) + H_r(z) \quad (\text{S27a})$$

(see eq. 22a and eq. 34a-c in Ohtsuki et al., 2020). The first,

$$H_w(z) = \frac{1}{2} \sum_{s \in \Omega} \sum_{s' \in \Omega} v_{s'}(z) \times \left[\frac{\partial^2 w_{s'|s,1}}{\partial z_1^2} + (n-1)r_{2,s}(z) \left\{ \frac{\partial^2 w_{s'|s,1}}{\partial z_2^2} + 2 \frac{\partial^2 w_{s'|s,1}}{\partial z_1 \partial z_2} \right\} + (n-1)(n-2)r_{3,s}(z) \frac{\partial^2 w_{s'|s,1}}{\partial z_2 \partial z_3} \right] p_s(z), \quad (\text{S27b})$$

consists of direct and relatedness-weighted indirect second-order effects of the trait on fitness, where $r_{3,s}(z)$ is threeway relatedness: the probability that three individuals from the same patch in state s are identical-by-

descent in a population monomorphic for z ; the second,

$$H_p(z) = \sum_{s \in \Omega} \sum_{s' \in \Omega} v_{s'}(z) \left[\frac{\partial w_{s'|s,1}}{\partial z_1} + (n-1)r_{2,s}(z) \frac{\partial w_{s'|s,1}}{\partial z_2} \right] p_s^{(1)}(z), \quad (\text{S27c})$$

depends on the first-order effect $p_s^{(1)}(z)$ of a trait change on the probability that a carrier of this change is in a patch of type s ; and finally, the third,

$$H_r(z) = \sum_{s \in \Omega} \sum_{s' \in \Omega} v_{s'}(z) \left[(n-1)r_{2,s}^{(1)}(z) \frac{\partial w_{s'|s,1}}{\partial z_2} \right] p_s(z), \quad (\text{S27d})$$

captures first-order effects $r_{2,s}^{(1)}(z)$ of the trait on relatedness (i.e., the first-order effect of a trait change on the probability that a randomly sampled neighbor carrier of this change in a patch of type s also expresses the trait change).

Threeway relatedness is found by solving the coalescent recursion,

$$r_{3,s}(z) = \gamma^3 r_{3,s}(z) + 3\gamma^2(1-\gamma)(1-d_s(z))r_{2;3,s}^R(z) + (1-\gamma)^2(1-d_s(z))^2 [3\gamma + (1-\gamma)(1-d_s(z))] r_{3,s}^R(z), \quad (\text{S28})$$

where

$$r_{2;3,s}^R(z) = \frac{2}{n} r_{2,s}(z) + \frac{n-2}{n} r_{3,s}(z) \quad (\text{S29})$$

is the probability that three individuals sampled randomly, two without replacement and one with replacement, from the same patch in state s are identical-by-descent, and

$$r_{3,s}^R(z) = \frac{1}{n^2} + 3 \frac{1}{n} \frac{(n-1)}{n} r_{2,s}(z) + \frac{(n-1)}{n} \frac{(n-2)}{n} r_{3,s}(z), \quad (\text{S30})$$

is the probability that three individuals sampled with replacement from the same patch in state s are identical-by-descent. We do not present here the explicit solution of eq. (S28) even though it is straightforward to obtain, as the solution is complicated (see eqs. F32 of Ohtsuki et al., 2020 for this solution that was obtained by a different method but agrees with the present one). Eq. (S27) further depends on the trait effect on the distribution in patch states, which has been shown to be such that

$$v_{s'}(z) p_s^{(1)}(z) = \left(\frac{1}{(1/n) - \phi_{s|s}^p(z)} \left[\frac{\partial \phi_{s|s}^p(z_1, \mathbf{z}_{-1}, z)}{\partial z_1} + (n-1)r_{2,s}(z) \frac{\partial \phi_{s|s}^p(z_1, \mathbf{z}_{-1}, z)}{\partial z_2} \right] - \sum_{s'' \in \Omega} \frac{1}{(1/n) - \phi_{s''|s''}^p(z)} \left[\frac{\partial \phi_{s|s}^p(z_1, \mathbf{z}_{-1}, z)}{\partial z_1} + (n-1)r_{2,s''}(z) \frac{\partial \phi_{s''|s''}^p(z_1, \mathbf{z}_{-1}, z)}{\partial z_2} \right] \right) v_{s'}(z) p_s(z), \quad (\text{S31})$$

(eq. 43 in Ohtsuki et al., 2020), as well as the trait effect on relatedness, which can be computed as,

$$r_{2,s}^{(1)}(z) = \frac{2n^2 r_{2,s}(z) \left[\gamma + (1-\gamma) n \phi_{s|s}^p(z) \right]}{2\gamma n \phi_{s|s}^p(z) + (1-\gamma) \left(n \phi_{s|s}^p(z) \right)^2} \left(r_{2,s}^R(z) \frac{\partial \phi_{s|s}^p(z_1, \mathbf{z}_{-1}, z)}{\partial z_1} + (n-1) r_{2;3,s}^R(z) \frac{\partial \phi_{s|s}^p(z_1, \mathbf{z}_{-1}, z)}{\partial z_2} \right) \quad (\text{S32})$$

(eq. 44 in Ohtsuki et al., 2020).

S2.3.3 Disruptive selection coefficient with fecundity effects

Plugging into eq. (S27) the expression for individual fitness $w_{s'|s}(z_1, z_{-1}, z)$ as well as its different components that we have derived for our model in Appendix A, we find after some re-arrangements that the coefficient of disruptive selection can be expressed as the average over patch states of three quantities that mirror the three terms of eq. (S27a),

$$H(z) = \sum_{s \in \Omega} (1 - \gamma) (H_{w,s}(z) + H_{p,s}(z) + H_{r,s}(z)) K_s(z) \pi_s \quad (\text{S33a})$$

where $K_s(z)$ is given by eq. (S25). Those three quantities are,

$$\begin{aligned} H_{w,s}(z) &= \frac{1}{2} \left[\left(\frac{\partial^2 f_{s,1}}{\partial z_1^2} + (n-1) r_{2,s}(z) \left(2 \frac{\partial^2 f_{s,1}}{\partial z_1 \partial z_2} + \frac{\partial^2 f_{s,1}}{\partial z_2^2} \right) + (n-1)(n-2) r_{3,s}(z) \frac{\partial^2 f_{s,1}}{\partial z_2 \partial z_3} \right) \right. \\ &\quad \left. - \Phi_s(z)^2 \left\{ r_{2,s}^R(z) \left(2 \frac{\partial f_{s,1}}{\partial z_1} \bar{F}_s(z) + \frac{\partial^2 f_{s,1}}{\partial z_1^2} + (n-1) \frac{\partial^2 f_{s,1}}{\partial z_2^2} \right) \right. \right. \\ &\quad \left. \left. + (n-1) r_{2:3,s}^R(z) \left(2 \frac{\partial f_{s,1}}{\partial z_2} \bar{F}_s(z) + 2 \frac{\partial^2 f_{s,1}}{\partial z_1 \partial z_2} + (n-2) \frac{\partial^2 f_{s,1}}{\partial z_2 \partial z_3} \right) \right\} \right] + \Phi_s(z)^3 r_{3,s}^R(z) \bar{F}_s(z)^2 \quad (\text{S33b}) \\ H_{p,s}(z) &= \frac{1 - d_s(z)}{d_s(z)} \left(F_s(z) - r_{2,s}^R(z) \Phi_s(z) \bar{F}_s(z) \right) \left(F_s(z) - r_{2,s}^R(z) \Phi_s(z)^2 \bar{F}_s(z) \right) \\ H_{r,s}(z) &= (n-1) r_{2,s}^{(1)}(z) \left(\frac{\partial f_{s,1}}{\partial z_2} - \frac{1}{n} \Phi_s(z)^2 \bar{F}_s(z) \right), \end{aligned}$$

where we have used notations introduced in sections S2.2 and S2.3.2 (see eqs. I13-I17 and H13-H17 in Ohtsuki et al., 2020 for more general results on the coefficient of disruptive selection on traits with fecundity effects). Further, substituting for the philopatric component of fitness (eqs. S4, S8) into (S32), we obtain that the trait effect on relatedness can be expressed in terms of fecundity effects as

$$r_{2,s}^{(1)}(z) = 2n r_{2,s}(z) \frac{\gamma + (1 - \gamma)(1 - d_s(z))}{2\gamma + (1 - \gamma)(1 - d_s(z))} \left[r_{2,s}^R(z) \frac{\partial f_{s,1}}{\partial z_1} + (n-1) r_{2:3,s}^R(z) \frac{\partial f_{s,1}}{\partial z_2} - r_{3,s}^R(z) \Phi_s(z) \bar{F}_s(z) \right]. \quad (\text{S34})$$

S3 Analyses

In this Appendix, we use the framework described in Appendix S2 to investigate the evolution of the consumer trait z and derive our results presented in the main text.

S3.1 Baseline scenario: long exploitation time

As a baseline, we assume that the time for consumption T within generations is long, or more specifically, long enough so that individuals have time to consume all available resources. This assumption allows our mathematical analysis to go further.

S3.1.1 Fecundity

Letting $T \rightarrow \infty$ in eqs. (5) and (I.C), we obtain that the fecundity of the focal individual simplifies to

$$f_s(z_1, z_{-1}) = k\beta R \sum_{j=1}^{n_R} \pi_{j|s} \frac{\alpha(z_1, q_j)}{\sum_{k=1}^n \alpha(z_k, q_j)}. \quad (\text{S35})$$

In this case, the sum of the fecundities of all individuals in the patch reads as

$$\sum_{i=1}^n f_s(z_i, z_{-i}) = k\beta R \sum_{j=1}^{n_R} \pi_{j|s} \sum_{i=1}^n \frac{\alpha(z_i, q_j)}{\sum_{k=1}^n \alpha(z_i, q_j)} = k\beta R = f_{\max}, \quad (\text{S36})$$

i.e., each patch produces the same number of offspring $f_{\max} = k\beta R$ (which is the maximum possible fecundity for an individual in the presence of trait variation). Selection therefore is always soft in this model (the case of hard selection is explored later).

In a population monomorphic for z (where $z_i = z$), the fecundity of an individual in a patch in state s is then simply,

$$f_s(z) = \frac{f_{\max}}{n}, \quad (\text{S37})$$

which is thus also equal to the average fecundity in the population,

$$f(z) = \sum_{s \in \Omega} \pi_s f_s(z) = \frac{f_{\max}}{n}. \quad (\text{S38})$$

As a result, the coefficient of variation in fecundity across patch types vanishes:

$$C_{v,f}(z) = \sqrt{\sum_{s \in \Omega} \pi_s \left(\frac{f_s(z)}{f(z)} - 1 \right)^2} = 0. \quad (\text{S39})$$

This further entails that the quantity $K_s(z)$ (eq. S25), which is relevant to both selection coefficients (eqs. S19 and S27) reduces to

$$K_s(z) = 1. \quad (\text{S40})$$

Relative fecundity of a focal individual, meanwhile, is obtained by substituting eq. (S35) and eq. (S37) into eq. (S21) to get

$$f_{s,1} = \frac{f_s(z_1, z_{-1})}{f_s(z)} = \sum_{j=1}^{n_R} \pi_{j|s} \frac{\alpha(z_1, q_j)}{\sum_{k=1}^n \alpha(z_k, q_j) / n}. \quad (\text{S41})$$

We can then use the above quantities to investigate how selection shapes the consumer trait z according to the framework described in Appendix S2.

S3.1.2 Directional selection

Substituting eq. (3), namely, $\alpha(z_i, q_j) = \exp\left(-\frac{(z_i - q_j)^2}{2\sigma_g^2}\right)$, into eq. (S41), we find that the direct (relative) fecundity effect is

$$\frac{\partial f_{s,1}}{\partial z_1} = - \sum_{j=1}^{n_R} \pi_{j|s} \frac{n-1}{n} \frac{z - q_j}{\sigma_g^2} = - \frac{n-1}{n} \frac{z - \bar{q}_s}{\sigma_g^2}, \quad (\text{S42})$$

where we recall that $\bar{q}_s = \sum_{j=1}^{n_R} \pi_{j|s} q_j$ is the average resource property in a patch of type s . Similarly, the indirect fecundity effect reads as

$$\frac{\partial f_{s,1}}{\partial z_2} = \frac{1}{n} \frac{z - \bar{q}_s}{\sigma_g^2}. \quad (\text{S43})$$

Accordingly, the sum of the direct and relatedness-weighted indirect fecundity effects (eq. S20) is

$$F_s(z) = - \frac{n-1}{n} \frac{z - \bar{q}_s}{\sigma_g^2} [1 - r_2], \quad (\text{S44})$$

where pairwise relatedness r_2 here is independent from the patch state s and the evolving trait z , i.e.,

$$r_2 = r_{2,z}(z) = \frac{2\gamma(1-m) + (1-\gamma)(1-m)^2}{n(1+\gamma) - 2\gamma(n-1)(1-m) - (1-\gamma)(n-1)(1-m)^2} \quad (\text{S45})$$

for all patch states s (to see this, substitute eqs. S37 and S38 into eq. S16 which is in turn substituted into eq. S17). The total fecundity effect (eq. S23) meanwhile vanishes,

$$\bar{F}_s(z) = 0. \quad (\text{S46})$$

Substituting eqs. (S44) and (S46) into the selection gradient eq. (S19) and using eq. (S40), we obtain

$$S(z) = - \sum_{s \in \Omega} (1-\gamma) \pi_s \frac{n-1}{n} \frac{z - \bar{q}_s}{\sigma_g^2} [1 - r_2] = - [1 - r_2] (1-\gamma) \frac{n-1}{n} \frac{z - \bar{q}}{\sigma_g^2}, \quad (\text{S47})$$

where recall $\bar{q} = \sum_{s \in \Omega} \pi_s \bar{q}_s$ is the global average resource property. It is immediate from eq. (S47) that the unique singular strategy z^* (eq. S10) is

$$z^* = \bar{q} \quad (\text{S48})$$

and that this strategy is convergence stable (eq. S11) since

$$\left. \frac{dS(z)}{dz} \right|_{z=z^*} = - [1 - r_2] (1-\gamma) \frac{n-1}{n} \frac{1}{\sigma_g^2} < 0. \quad (\text{S49})$$

S3.1.3 Disruptive selection

We now compute the disruptive selection coefficient from eq. (S33). To that end, consider first the direct second-order fecundity effect at the singular strategy $z^* = \bar{q}$:

$$\frac{\partial^2 f_{s,1}}{\partial z_1^2} = \sum_{j=1}^{n_R} \pi_{j|s} \frac{n-1}{n} \frac{1}{\sigma_g^2} \left(\frac{n-2}{n} \frac{(q_j - \bar{q})^2}{\sigma_g^2} - 1 \right), \quad (\text{S50})$$

which averaged over environmental states as in eq. (S33), becomes

$$\sum_{s \in \Omega} (1-\gamma) K_s(z) \frac{\partial^2 f_{s,1}}{\partial z_1^2} \pi_s = (1-\gamma) \frac{n-1}{n} \frac{1}{\sigma_g^2} \left(\frac{n-2}{n} \frac{\sigma_{r,w}^2 + \sigma_{r,b}^2}{\sigma_g^2} - 1 \right), \quad (\text{S51})$$

where we used $K_s(z) = 1$ (eq. (S40)) and the fact that $\sum_{s \in \Omega} \sum_{j=1}^{n_R} \pi_{j|s} \pi_s (q_j - \bar{q})^2 = \sigma_{r,w}^2 + \sigma_{r,b}^2 = \sigma_r^2$ is the total variance in resource property. Following the same procedure as the one used for eqs. (S50)-(S51), we readily obtain the remaining relevant second-order fecundity effects for the disruptive selection coefficient (eq. S33):

$$\begin{aligned} \sum_{s \in \Omega} (1-\gamma) K_s(z) \frac{\partial^2 f_{s,1}}{\partial z_2^2} \pi_s &= (1-\gamma) \frac{1}{n} \frac{1}{\sigma_g^2} \left(1 - \frac{n-2}{n} \frac{\sigma_{r,w}^2 + \sigma_{r,b}^2}{\sigma_g^2} \right) \\ \sum_{s \in \Omega} (1-\gamma) K_s(z) \frac{\partial^2 f_{s,1}}{\partial z_1 \partial z_2} \pi_s &= -(1-\gamma) \frac{1}{n} \frac{1}{\sigma_g^2} \frac{n-2}{n} \frac{\sigma_{r,w}^2 + \sigma_{r,b}^2}{\sigma_g^2} \\ \sum_{s \in \Omega} (1-\gamma) K_s(z) \frac{\partial^2 f_{s,1}}{\partial z_2 \partial z_3} \pi_s &= (1-\gamma) \frac{2}{n} \frac{1}{\sigma_g^2} \frac{1}{n} \frac{\sigma_{r,w}^2 + \sigma_{r,b}^2}{\sigma_g^2}. \end{aligned} \quad (\text{S52})$$

Using eqs. (S51)-(S52), we find that the two total effects,

$$\begin{aligned} \sum_{s \in \Omega} (1-\gamma) K_s(z) \left(\frac{\partial^2 f_{s,1}}{\partial z_1^2} + (n-1) \frac{\partial^2 f_{s,1}}{\partial z_2^2} \right) \pi_s &= 0, \\ \sum_{s \in \Omega} (1-\gamma) K_s(z) \left(2 \frac{\partial^2 f_{s,1}}{\partial z_1 z_2} + (n-2) \frac{\partial^2 f_{s,1}}{\partial z_2 z_3} \right) \pi_s &= 0, \end{aligned} \quad (\text{S53})$$

reduce to zero. As a result (and using eqs. (S44)-(S46)), the first term $H_w(z) = \sum_{s \in \Omega} (1-\gamma) K_s(z) H_{w,s}(z) \pi_s$ of the disruptive selection coefficient reduces to

$$H_w(z) = (1-\gamma) \frac{n-1}{n} \frac{1}{\sigma_g^2} \frac{1}{2} \left(\frac{n-2}{n} (1-L) \frac{\sigma_{r,b}^2 + \sigma_{r,w}^2}{\sigma_g^2} - (1-r_2) \right), \quad (\text{S54})$$

where

$$L = 3r_2 - 2r_3 \quad (\text{S55})$$

is the probability that at least two out of three individuals are identical-by-descent (so that $1-L$ is the probability that none out of three are identical-by-descent), with

$$r_3 = r_{3,s}(z) \quad \text{for all } s, \quad (\text{S56})$$

as the probability of identity-by-descent of three individuals from the same patch. Like pairwise relatedness (eq. S45), r_3 is independent from patch state and the evolving trait here. It is found by solving

$$r_3 = \gamma^3 r_3 + 3\gamma^2(1-\gamma)(1-m)r_{2:3}^R + (1-\gamma)^2(1-m)^2[3\gamma + (1-\gamma)(1-m)]r_3^R, \quad (\text{S57})$$

where

$$\begin{aligned} r_{2:3}^R &= \frac{2}{n}r_2 + \frac{n-2}{n}r_3 \\ r_3^R &= \frac{1}{n^2} + 3\frac{1}{n}\frac{(n-1)}{n}r_2 + \frac{(n-1)}{n}\frac{(n-2)}{n}r_3 \end{aligned} \quad (\text{S58})$$

(obtained by substituting eqs. S37 and S38 into eq. S16 which is in turn substituted into eq. S28).

Plugging eqs. (S16), (S34), and eqs. (S43)-(S46) into eq. (S33), we find, after some re-arrangements, that the other two terms of the disruptive selection coefficient, $H_p(z) = \sum_{s \in \Omega} (1-\gamma)K_s(z)H_{p,s}(z)\pi_s$ and $H_r(z) = \sum_{s \in \Omega} (1-\gamma)K_s(z)H_{r,s}(z)\pi_s$, read as

$$H_p(z) = (1-\gamma)\frac{(n-1)}{n}\frac{1}{\sigma_g^2}\left(\frac{(n-1)}{n}\frac{(1-m)}{m}(1-r_2)^2\frac{\sigma_{r,b}^2}{\sigma_g^2}\right) \quad (\text{S59})$$

and

$$H_r(z) = -(1-\gamma)\frac{(n-1)}{n}\frac{1}{\sigma_g^2}\left(2(n-1)\frac{(1-(1-\gamma)m)}{(1-(1-\gamma)m+\gamma)}r_2\left(\frac{1-L}{n} + r_2 - r_3\right)\frac{\sigma_{r,b}^2}{\sigma_g^2}\right). \quad (\text{S60})$$

Summing eqs. (S54), (S59), and (S60), we eventually obtain that the coefficient of disruptive selection at $z = \bar{q}$ can be expressed as

$$H(z) = \frac{1-\gamma}{\sigma_g^2}\frac{n-1}{n}\left(\chi_1\frac{\sigma_{r,b}^2}{\sigma_g^2} + \chi_2\frac{\sigma_{r,w}^2}{\sigma_g^2} - \chi_3\right), \quad (\text{S61})$$

where

$$\begin{aligned} \chi_1 &= \frac{n-1}{n}\frac{1-m}{m}(1-r_2)^2 - 2(n-1)\frac{1-(1-\gamma)m}{1-(1-\gamma)m+\gamma}\left(\frac{1-L}{n} + r_2 - r_3\right)r_2 + \chi_2 \\ \chi_2 &= \frac{n-2}{n}\frac{1}{2}(1-L) \\ \chi_3 &= \frac{1-r_2}{2}. \end{aligned} \quad (\text{S62})$$

Substituting eq. (S61) into the branching condition, $H(z) > 0$, we obtain after some algebra condition (7) of the main text, namely

$$\frac{\sigma_r^2}{\sigma_g^2}(\chi_b E_{ST} + \chi_w(1 - E_{ST})) > 1, \quad (\text{S63})$$

where

$$\chi_b = \frac{\chi_1}{\chi_3} \quad \text{and} \quad \chi_w = \frac{\chi_2}{\chi_3}. \quad (\text{S64})$$

After inserting the expressions for the relatedness coefficients into eq. (S62) we obtain from eq. (S64) the defi-

nitions given by eq. (8) in the main text for χ_b and χ_w in the limit where patches are large and dispersal is weak (where $n \rightarrow \infty$ and $m \rightarrow 0$ such that nm remains constant). Note that when dispersal is complete ($m = 1$) so that individuals do not compete with related individuals ($r_2 = 0$ and $r_3 = 0$), χ_b and χ_w in eq. (S64) both reduce to

$$\chi_b = \chi_w = 1 - \frac{2}{n}, \quad (\text{S65})$$

which increases to one as patch size increases.

S3.2 Short exploitation time

Here we analyse our model when exploitation time T is short and derive the results described in section "Hard selection and alternative routes to polymorphism" of the main text.

S3.2.1 Fecundity

To obtain the fecundity of a focal individual expressing trait z_1 in a patch of type s , we first Taylor-expand eq. (I.C) from Box I of the main text around $T = 0$:

$$E_s(z_1, \mathbf{z}_{-1}) = \beta \sum_j R_{j,s}(0) T \alpha(z_1, q_j) + \mathcal{O}(T^2). \quad (\text{S66})$$

This expression depends only on trait z_1 expressed by the focal individual (i.e., it is independent of the trait values of other patch members). This is because exploitation time is too short for competition to affect the focal's resource uptake. Nonetheless, there is still competition for breeding spots whose outcome depends on the amount of resources collected.

Since the general case with arbitrary resource distribution (given by $\pi_{j|s}$ and π_s) is too complicated, we assume that resources within patches follow a Normal distribution. In other words, we assume that there is an effectively infinite number of resource types that are continuously distributed such that the quantity of a resource j with property q_j in a patch of type s is,

$$R_{j,s}(0) = R \frac{1}{\sqrt{2\pi\sigma_{r,w}^2}} \exp\left(-\frac{1}{2} \frac{(q_j - \bar{q}_s)^2}{\sigma_{r,w}^2}\right), \quad (\text{S67})$$

where \bar{q}_s is the average resource property in a patch of type s (eq. S67 is the continuous analogue to eq. I.B of the main text). The fecundity of a focal individual is then calculated by plugging eq. (S67) into eq. (S66), which in turn is integrated over all resource types (rather than summed as in eq. 5 since the resource distribution is

continuous), i.e.

$$f_s(z_1, z_{-1}) = f_{\max} \int_{-\infty}^{\infty} \frac{1}{\sqrt{2\pi\sigma_{r,w}^2}} \exp\left(-\frac{1}{2} \frac{(q_j - \bar{q}_s)^2}{\sigma_{r,w}^2}\right) \alpha(z_1, q_j) dq_j = f_{\max} \frac{\sqrt{\sigma_g^2}}{\sqrt{\sigma_g^2 + \sigma_{r,w}^2}} \exp\left(-\frac{(z_1 - \bar{q}_s)^2}{2(\sigma_g^2 + \sigma_{r,w}^2)}\right), \quad (\text{S68})$$

where $f_{\max} = k\beta RT$ is the maximum fecundity in this model and the function $\alpha(z_1, q_j)$ is given by eq. (3). From eq. (S68), fecundity in a patch of type s for a population monomorphic for z is then

$$f_s(z) = f_{\max} \frac{\sqrt{\sigma_g^2}}{\sqrt{\sigma_g^2 + \sigma_{r,w}^2}} \exp\left(-\frac{(z - \bar{q}_s)^2}{2(\sigma_g^2 + \sigma_{r,w}^2)}\right) \quad (\text{S69})$$

so that we obtain

$$f_{s,1} = \frac{f_s(z_1, z_{-1})}{f_s(z)} = \exp\left(-\frac{(z_1 - \bar{q}_s)^2 - (z - \bar{q}_s)^2}{2(\sigma_g^2 + \sigma_{r,w}^2)}\right), \quad (\text{S70})$$

for the relative fecundity of the focal individual.

To derive further relevant quantities to our analysis, we make use of our assumption given in section "Hard selection and alternative routes to polymorphism" that there are two patch types, 1 and 2. These occur in equal frequency ($\pi_1 = \pi_2 = 1/2$) and differ in the average property of the resources they hold according to

$$\begin{aligned} \bar{q}_1 &= \bar{q} - \sigma_{r,b} \\ \bar{q}_2 &= \bar{q} + \sigma_{r,b}, \end{aligned} \quad (\text{S71})$$

where \bar{q} is the global average of resource property so that $\sigma_{r,b}^2 = (\bar{q}_1 - \bar{q})^2 / 2 + (\bar{q}_2 - \bar{q})^2 / 2$ is the between patch variance in resource property, as required. In this case, the average fecundity in a monomorphic population reads as,

$$f(z) = f_{\max} \frac{1}{2} \frac{\sqrt{\sigma_g^2}}{\sqrt{\sigma_g^2 + \sigma_{r,w}^2}} \left[\exp\left(-\frac{(z - \bar{q} - \sigma_{r,b})^2}{2(\sigma_g^2 + \sigma_{r,w}^2)}\right) + \exp\left(-\frac{(z - \bar{q} + \sigma_{r,b})^2}{2(\sigma_g^2 + \sigma_{r,w}^2)}\right) \right]. \quad (\text{S72})$$

Plugging eqs. (S69) and (S72) into eq. (S26), we obtain

$$C_{v,f}^2(z) = \tanh\left(-\frac{(z - \bar{q})\sigma_{r,b}}{\sigma_g^2 + \sigma_{r,w}^2}\right)^2 \quad (\text{S73})$$

for the coefficient of variation in fecundity in a monomorphic population, where \tanh is the hyperbolic tangent function.

S3.2.2 Directional selection

To compute the selection gradient $S(z)$ (from eq. S19), we first obtain from eq. (S70) the direct (relative) fecundity effect,

$$\frac{\partial f_{s,1}}{\partial z_1} = -\frac{z - \bar{q}_s}{\sigma_g^2 + \sigma_{r,w}^2}, \quad (\text{S74})$$

as well as the indirect fecundity effect,

$$\frac{\partial f_{s,1}}{\partial z_2} = 0. \quad (\text{S75})$$

Accordingly, the two relevant total effects $F_s(z)$ (eq. S20) and $\bar{F}_s(z)$ (eq. S23) that appear in the selection gradient reduce to

$$F_s(z) = \bar{F}_s(z) = \frac{\partial f_{s,1}}{\partial z_1}. \quad (\text{S76})$$

The selection gradient (eq. S19) thus simplifies to

$$S(z) = \frac{1-\gamma}{2} \sum_{s=1}^2 K_s(z) \left(-\frac{z - \bar{q}_s}{\sigma_g^2 + \sigma_{r,w}^2} \right) (1 - \Phi_s(z)^2 r_{2,s}^R(z)), \quad (\text{S77})$$

where we have used the assumption that there are two patch types occurring at equal frequency ($\pi_1 = \pi_2 = 1/2$). The mathematical expressions for $K_s(z)$, $\Phi_s(z)$, and $r_{2,s}^R(z)$ in eq. (S77) are then found using the different fecundity functions derived in section S3.2.1 (plugged into eqs. S15-S17, S25 and S22). Although straightforward, this operation leads to an unsightly equation that is too complex to give much intuition on directional selection. We therefore do not present this equation and rather analyse the selection gradient numerically. This generates our results shown in Fig. 5 (i.e., we find singular strategies z^* and test whether these are convergence stable using eqs. S10 and S11 for various parameter combinations shown in Fig. 5).

To show that $z^* = \bar{q}$ is a singular strategy, consider first that when the population is monomorphic for $z = \bar{q}$, one has $K_s(z) = 1$, as well as,

$$1 - \Phi_s(z)^2 r_{2,s}^R(z) = 1 - (1-m)^2 \left(\frac{1}{n} + \frac{n-1}{n} r_2 \right) \quad (\text{S78})$$

with r_2 from eq. (S45) (when $z = \bar{q}$). The expression for the selection gradient (eq. S77) then reduces to

$$S(z) = -(1-\gamma) \left(1 - (1-m)^2 \left(\frac{1}{n} + \frac{n-1}{n} r_2 \right) \right) \frac{(z - \bar{q})}{\sigma_g^2 + \sigma_{r,w}^2}, \quad (\text{S79})$$

indicating that $z^* = \bar{q}$ is always a singular strategy (where $S(z) = 0$). Our numerical analysis of the selection gradient, however, reveals that $z^* = \bar{q}$ is not always convergence stable. When it is convergence stable, it is the only singular strategy. But when $z^* = \bar{q}$ is not convergence stable, two additional singular strategies exist, one close to \bar{q}_1 and another close to \bar{q}_2 (Fig. 5). In this case convergence to either singularity depends on initial condition.

S3.2.3 Disruptive selection

We now compute the disruptive selection coefficient (eq. S33). To do so, we first obtain from eq. (S70) the direct second-order effect,

$$\frac{\partial^2 f_{s,1}}{\partial z_1^2} = \left(\frac{z - \bar{q}_s}{\sigma_g^2 + \sigma_{r,w}^2} \right)^2 - \frac{1}{\sigma_g^2 + \sigma_{r,w}^2}. \quad (\text{S80})$$

From eq. (S70) still, we further see that all indirect second-order effects reduce to zero,

$$\frac{\partial^2 f_{s,1}}{\partial z_2^2} = \frac{\partial^2 f_{s,1}}{\partial z_1 \partial z_2} = \frac{\partial^2 f_{s,1}}{\partial z_2 \partial z_3} = 0. \quad (\text{S81})$$

Using eqs. (S74)-(S76) and (S80)-(S81), eq. (S33b) becomes,

$$\begin{aligned} H_{w,s}(z) &= \frac{1}{2} \left[\left(\frac{z - \bar{q}_s}{\sigma_g^2 + \sigma_{r,w}^2} \right)^2 (1 - 3\Phi_s(z)^2 r_{2,s}^R(z) + 2\Phi_s(z)^3 r_{3,s}^R(z)) - \frac{1}{\sigma_g^2 + \sigma_{r,w}^2} (1 - \Phi_s(z)^2 r_{2,s}^R(z)) \right] \\ H_{p,s}(z) &= \frac{1 - d_s(z)}{d_s(z)} \left(\frac{z - \bar{q}_s}{\sigma_g^2 + \sigma_{r,w}^2} \right)^2 (1 - \Phi_s(z) r_{2,s}^R(z)) (1 - \Phi_s(z)^2 r_{2,s}^R(z)) \\ H_{r,s}(z) &= -2(n-1) r_{2,s}(z) \frac{\gamma + (1-\gamma)(1 - d_s(z))}{2\gamma + (1-\gamma)(1 - d_s(z))} \Phi_s(z)^2 (r_{2,s}^R(z) - \Phi_s(z) r_{3,s}^R(z)) \left(\frac{z - \bar{q}_s}{\sigma_g^2 + \sigma_{r,w}^2} \right)^2. \end{aligned} \quad (\text{S82})$$

The coefficient of disruptive selection is then found by plugging eq. (S82) into eq. (S33) and using the different fecundity functions derived in section S3.2.1 to compute the relevant quantities $r_{2,s}^R(z)$ (eq. S15), $d_s(z)$ (eq. S16), $r_{2,s}(z)$ (eq. S17), $K_s(z)$ (eq. S25), $\Phi_s(z)$ (eq. S22), $r_{3,s}^R(z)$ (eq. S30), $F_s(z)$ and $\bar{F}_s(z)$ (eq. S76).

The coefficient of disruptive selection is complicated but we can get further insights for the case where the population has converged to match the global average resource property, i.e., when $z^* = \bar{q}$ is convergence stable. In this case, relative fecundity reduces to

$$\frac{f_s(z)}{f(z)} = 1 \quad (\text{S83})$$

for both states $s = 1, 2$ (using eqs. S69, S71 and S72). As a consequence, many relevant quantities that appear in eq. (S82) simplify. In particular, $d_s(z) = m$ and relatedness coefficients no longer depend on patch state,

satisfying eqs. (S45) and (S56)-(S58). We thus obtain,

$$\begin{aligned}
 H_w(z) &= \sum_{s \in \Omega} (1 - \gamma) K_s(z) H_{w,s}(z) \pi_s \\
 &= \frac{1}{2} \frac{1 - \gamma}{(\sigma_g^2 + \sigma_{r,w}^2)} \left[\frac{\sigma_{r,b}^2}{(\sigma_g^2 + \sigma_{r,w}^2)} (1 - 3(1 - m)^2 r_2^R + 2(1 - m)^3 r_3^R) - (1 - (1 - m)^2 r_2^R) \right] \\
 H_p(z) &= \sum_{s \in \Omega} (1 - \gamma) K_s(z) H_{p,s}(z) \pi_s \\
 &= \frac{1 - \gamma}{(\sigma_g^2 + \sigma_{r,w}^2)} \frac{\sigma_{r,b}^2}{(\sigma_g^2 + \sigma_{r,w}^2)} \frac{1 - m}{m} (1 - (1 - m) r_2^R) (1 - (1 - m)^2 r_2^R) \\
 H_r(z) &= \sum_{s \in \Omega} (1 - \gamma) K_s(z) H_{r,s}(z) \pi_s \\
 &= -2 \frac{1 - \gamma}{\sigma_g^2 + \sigma_{r,w}^2} (n - 1) r_2 \frac{\gamma + (1 - \gamma)(1 - m)}{2\gamma + (1 - \gamma)(1 - m)} (1 - m)^2 (r_2^R - (1 - m) r_3^R) \frac{\sigma_{r,b}^2}{(\sigma_g^2 + \sigma_{r,w}^2)},
 \end{aligned} \tag{S84}$$

for the three components of the coefficient of disruptive selection when $z = z^* = \bar{q}$. Summing these components yields,

$$H(z) = H_w(z) + H_p(z) + H_r(z) = \frac{1 - \gamma}{\sigma_g^2 + \sigma_{r,w}^2} \left(\chi_A \frac{\sigma_{r,b}^2}{\sigma_g^2 + \sigma_{r,w}^2} - \chi_C \right), \tag{S85}$$

for when $z = z^* = \bar{q}$ where

$$\begin{aligned}
 \chi_A &= \left(\frac{1}{2} (1 - 3(1 - m)^2 r_2^R + 2(1 - m)^3 r_3^R) + 2(n - 1) r_2 \frac{\gamma + (1 - \gamma)(1 - m)}{2\gamma + (1 - \gamma)(1 - m)} (1 - m)^2 (r_2^R - (1 - m) r_3^R) \right) \\
 \chi_C &= \frac{1}{2} (1 - (1 - m)^2 r_2^R).
 \end{aligned} \tag{S86}$$

From eq. (S85), we obtain the branching condition (9) of the main text, i.e., that $H(z) > 0$ is equivalent to

$$\frac{\sigma_r^2}{\sigma_g^2} (\chi_h E_{ST} - (1 - E_{ST})) > 1, \tag{S87}$$

where $\sigma_{r,b}^2 = \sigma_r^2 E_{ST}$, $\sigma_{r,w}^2 = \sigma_r^2 (1 - E_{ST})$ and

$$\chi_h = \frac{\chi_A}{\chi_C}. \tag{S88}$$

S3.2.4 Local competition

To investigate the impact of local competition when exploitation time is short, we assumed that density regulation additionally occurs before dispersal (between step 1) and 2) of the life cycle) so that the density of offspring within each patch is reduced to the same (large) offspring carrying capacity C (where $C \gg 1$). In this case, the

philopatric and dispersal components of individual fitness (Appendix S1.1) are now given by

$$\phi_{s|s}^p(z_1, \mathbf{z}_{-1}, z) = (1 - m) \frac{f_s(z_1, \mathbf{z}_{-1})}{\sum_{i=1}^n f_s(z_i, \mathbf{z}_{-i})}, \quad (\text{S89})$$

$$\phi_{s'|s}^d(z_1, \mathbf{z}_{-1}, z) = \pi_{s'} m \frac{f_s(z_1, \mathbf{z}_{-1})}{\sum_{i=1}^n f_s(z_i, \mathbf{z}_{-i})}, \quad (\text{S90})$$

so that they reduce to

$$\begin{aligned} \phi_{s'|s}^d(z) &= \pi_{s'} \frac{m}{n} \\ \phi_{s|s}^p(z) &= \frac{1 - m}{n} \end{aligned} \quad (\text{S91})$$

in a monomorphic population.

We can then repeat our derivation of the selection gradient $S(z)$ (from eq. S12) and the disruptive selection coefficient $H(z)$ (from eq. S27) using the above. Note that in this case, we find that in terms of fecundity effects, the selection gradient and coefficient of disruptive selection can still be expressed respectively as eqs. (S19) and (S33) except that

$$\Phi_s(z) = 1. \quad (\text{S92})$$

This is because the probability $\Phi_s(z)^2$ that two offspring born in the same patch of type s compete with one another is equal to one with density regulation occurring before dispersal. In addition, since the same number of offspring is produced in each patch, we have

$$K_s(z) = 1 \quad (\text{S93})$$

(as $f_s(z) = f(z)$ for all s).

Selection gradient. Using eq. (S92) and (S93), we obtain that the selection gradient is,

$$S(z) = \sum_{s \in \Omega} \pi_s (1 - \gamma) (1 - r_2^R) \frac{\bar{q}_s - z}{\sigma_g^2 + \sigma_{r,w}^2} = (1 - \gamma) (1 - r_2^R) \frac{\bar{q} - z}{\sigma_g^2 + \sigma_{r,w}^2}. \quad (\text{S94})$$

Eq. (S94) shows that $z^* = \bar{q}$ is the only singular strategy, which is also convergence stable as,

$$\left. \frac{dS(z)}{dz} \right|_{z=z^*} = -(1 - \gamma) (1 - r_2^R) \frac{1}{\sigma_g^2 + \sigma_{r,w}^2} < 0. \quad (\text{S95})$$

Disruptive selection. Similarly, we obtain that the three components of the coefficient of disruptive selection read as,

$$\begin{aligned}
 H_W(z) &= \sum_{s \in \Omega} (1 - \gamma) K_s(z) H_{W,s}(z) \pi_s \\
 &= \frac{1}{2} \frac{1 - \gamma}{(\sigma_g^2 + \sigma_{r,w}^2)} \left[\frac{\sigma_{r,b}^2}{(\sigma_g^2 + \sigma_{r,w}^2)} (1 - 3r_2^R + 2r_3^R) - (1 - r_2^R) \right] \\
 H_P(z) &= \sum_{s \in \Omega} (1 - \gamma) K_s(z) H_{P,s}(z) \pi_s \\
 &= \frac{1 - \gamma}{(\sigma_g^2 + \sigma_{r,w}^2)} \frac{\sigma_{r,b}^2}{(\sigma_g^2 + \sigma_{r,w}^2)} \frac{1 - m}{m} (1 - r_2^R)^2 \\
 H_I(z) &= \sum_{s \in \Omega} (1 - \gamma) K_s(z) H_{I,s}(z) \pi_s \\
 &= -2 \frac{1 - \gamma}{\sigma_g^2 + \sigma_{r,w}^2} (n - 1) r_2 \frac{\gamma + (1 - \gamma)(1 - m)}{2\gamma + (1 - \gamma)(1 - m)} (r_2^R - r_3^R) \frac{\sigma_{r,b}^2}{(\sigma_g^2 + \sigma_{r,w}^2)},
 \end{aligned} \tag{S96}$$

where $z = z^* = \bar{q}$ so that

$$H(z) = H_W(z) + H_P(z) + H_I(z) = \frac{1 - \gamma}{\sigma_g^2 + \sigma_{r,w}^2} \left(\chi_A \frac{\sigma_{r,b}^2}{\sigma_g^2 + \sigma_{r,w}^2} - \chi_C \right), \tag{S97}$$

where

$$\begin{aligned}
 \chi_A &= \left(\frac{1}{2} (1 - 3r_2^R + 2r_3^R) + \frac{1 - m}{m} (1 - r_2^R)^2 - 2(n - 1) r_2 \frac{\gamma + (1 - \gamma)(1 - m)}{2\gamma + (1 - \gamma)(1 - m)} (r_2^R - r_3^R) \right) \\
 \chi_C &= \frac{1}{2} (1 - r_2^R).
 \end{aligned} \tag{S98}$$

From eq. (S97), it is straightforward to obtain that $H(z) > 0$ if and only if,

$$\sigma_r^2 (\chi_b E_{ST} - (1 - E_{ST})) > \sigma_g^2, \tag{S99}$$

where

$$\chi_b = \frac{\chi_A}{\chi_C}. \tag{S100}$$

is identical to χ_b where exploitation time is long (eq. S64). Hence, the condition for the emergence of polymorphism is identical to when exploitation time is long and resources vary only between patches (i.e., S99 is identical to S63 when $E_{ST} = 1$).

S4 Individual-based simulations

To accompany our mathematical analysis, we used *Nemo-Age* (Cotto et al., 2020) to simulate a diploid population of hermaphrodites subdivided among 2,000 patches of two types ($s = 1, 2$) with equal frequency ($\pi_1 = \pi_2 = 1/2$; for the simulation code see Schmid et al., 2023). We fixed the global resource property to $\bar{q} = 50$.

Then patches of type 1 and 2 were characterized by a normal distribution of resources with mean $\bar{q}_1 = \bar{q} + \sigma_{r,b}$ and $\bar{q}_2 = \bar{q} - \sigma_{r,b}$, respectively, and variance $\sigma_{r,w}^2$ (the distribution was discretized into 51 equally sized bins to obtain $\pi_{j|s}$ for $j = 1, \dots, 51$ and $s = 1, 2$). We explored various resource distribution by varying within- ($\sigma_{r,w}^2$) and between-patch ($\sigma_{r,b}$) variance to obtain five degrees of resource differentiation between patches ($E_{ST}=0$, $E_{ST}=0.25$, $E_{ST}=0.5$, $E_{ST}=0.75$, $E_{ST}=1$) for two levels of the total resource variation ($\sigma_r^2=1$ and $\sigma_r^2=2$).

The life cycle in our simulations matched the one described in the main text (section "Population and life-cycle events") with the following events occurring each year: (1) Adults reproduced asexually making a number of offspring randomly drawn from a Poisson distribution with mean given by eq. (S35) (or eq. S68 depending on the scenario studied) with each offspring a clonal copy of its hermaphroditic parent. (2) Offspring dispersed to a randomly chosen, non-natal patch with probability m or remained philopatric with probability $1 - m$. (3) All adults died (so we assumed $\gamma=0$ in all our simulations corresponding to a Wright-Fisher process). (4) $n = 10$ offspring were randomly sampled in each patch to become the adults of the next year.

To investigate the effects of sexual reproduction (and generate Figs. 6), we assumed that, instead of step (1) above, hermaphrodite individuals mated randomly within patches. Specifically, we first picked the number of haploid eggs produced by each adult from a Poisson distribution with mean given by eq. (S35) (or eq. S68). Second, for each of these eggs, we picked an individual at random (with replacement) from the same patch to provide the fertilizing haploid sperm (so that an individual self-fertilizes with probability $1/n$). The offspring individual resulted from the fusion of these two gametes.

Each individual i expressed a consumer trait z_i that controlled the feeding rate and determined individual fecundity $f_s(z_i, z_{-i})$. The individual trait value was controlled by a single locus with additive allelic effects (so that an individual i with alleles $a_{1,i}$ and $a_{2,i}$ expressed phenotype $z_i = a_{1,i} + a_{2,i}$; note that there is no environmental effect on phenotype in our simulations). Mutations occurred with probability $\mu = 0.00001$, with an effect whose size was picked from a normal distribution $\mathcal{N}(0, 0.05)$ (and added to the existing allelic effect following the continuum-of-alleles model). In addition to the adaptive locus, each individual also carried an unlinked neutral locus that mutated according to the single-step mutational model (aimed at capturing microsatellite evolution): mutations occurred with probability $\mu = 0.00001$ and increased or decreased the allelic value by +1 or -1 (with reflective boundaries at 1 and 256). Recombination between selected and neutral loci took place only under sexual reproduction (as under asexual reproduction, individuals make a copy of themselves).

We ran the simulations for 2,000 years, recording relevant summary statistics every 25 years, and storing the phenotypes of the entire population at year 2,000. Differentiation in additive genetic effects of consumer traits (Q_{ST} , which is identical to phenotypic differentiation P_{ST} in our simulations since we assumed no environmental effects) was calculated as follows. Phenotypic variance within and between patches was computed from an analysis of variance using the *aov*-function from the *stats*-package in R (version 4.2.1, R Core Team, 2019). Additive genetic variance within populations was computed as $V_{G,w} = MS_{within}$ (the mean square within patches), the additive genetic variance between populations as $V_{G,b} = (MS_{between} - MS_{within}) / \eta_0$ with $\eta_0 = 10$

(where MS_{between} is the mean square between patches and η_0 is the average sample size per patch; e.g., see Storz et al., 2001; Martin et al., 2008). Then Q_{ST} was computed as $Q_{ST} = V_{G,b} / (V_{G,b} + V_{G,w})$ under clonal reproduction, and $Q_{ST} = V_{G,b} / (V_{G,b} + 2V_{G,w})$ under sexual reproduction. Note that in our model $V_{G,b} = V_{P,b}$ and $V_{G,w} = V_{P,w}$ as we do not have any environmental effects on phenotype expression. We computed differentiation in allele frequencies at the neutral locus F_{ST} with the *wc*-function of the *hierfstat*-package following the Weir-Cockerham approach (Goudet, 2005). Here, allele frequency differentiation over all alleles indexed u at the neutral locus is estimated from a weighted analysis of variance, that for a large number of large patches reduces to $F_{ST} = (\sum_u V_{F,b,u}) / (\sum_u V_{F,u})$, the between-patch variance in allele frequencies $V_{F,b,u}$ over the total variance $V_{F,u}$. The computation of F_{ST} with small patch sizes is more elaborate though (see Weir and Cockerham, 1984).

S5 Supplementary Figures

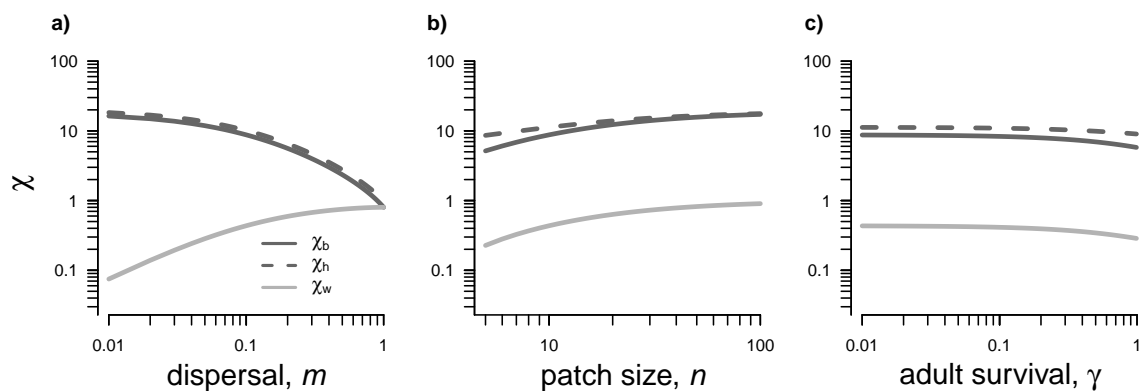


Figure S1: **The relative importance of local and spatial resource variation in promoting polymorphism.** The factors to spatial (χ_b , χ_h) and local (χ_w) resource variation that appear in the branching conditions (7) and (9) are plotted against dispersal m (a), patch size n (b), and adult survival γ (c). If not specified otherwise, the dispersal probability equals $m = 0.1$, the local patch size $n = 10$, and adult survival $\gamma = 0$. See eqs. (C28)-(C30) and eq. (C54) in Appendix for details.

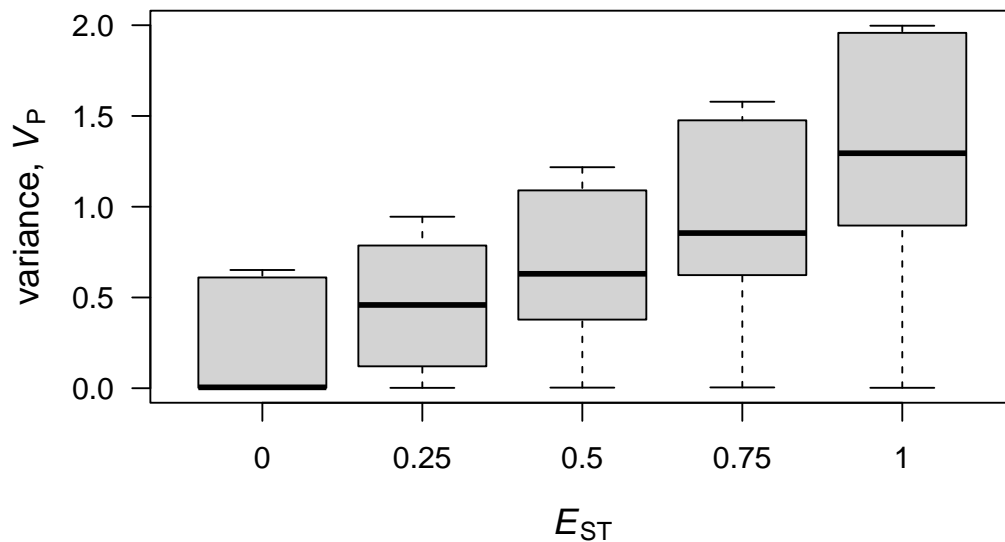


Figure S2: **Phenotypic variance according to resource differentiation among patches E_{ST} .** Box plots for the distribution of phenotypic variance V_P for five different levels of E_{ST} . Each box-plot is based on 22 simulations covering all the possible parameter combinations of: $\sigma_I^2 = 1, 2$, $m = 0.05, 0.1, 0.2, \dots, 1.0$. Fixed parameters: $\sigma_g^2 = 1$, $n = 10$, and $\gamma = 0$. Phenotypic variances are measured after 2,000 years of evolution during step 4) of the annual life cycle. The results show that phenotypic variance increases with E_{ST} .

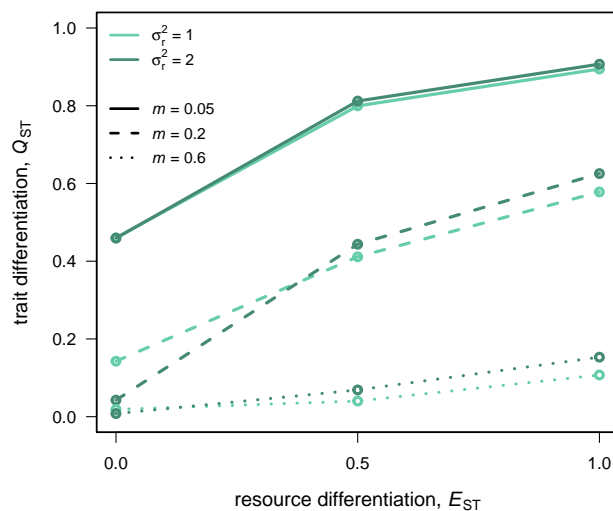


Figure S3: **Trait differentiation Q_{ST} as a function of resource differentiation E_{ST} .** Simulation results for a single replicate after 2,000 years for the evolved levels of consumer trait differentiation among patches against the underlying resource differentiation E_{ST} . We show results for two levels of the total resource variance ($\sigma_I^2 = 1, 2$; light and dark green) and three dispersal propensities ($m = 0.05, 0.2, 0.6$; solid, dashed and dotted lines). Fixed parameters: $\sigma_g^2 = 1$, $n = 10$, $\gamma = 0$. This indicates that trait differentiation Q_{ST} is positively associated with resource differentiation E_{ST} .

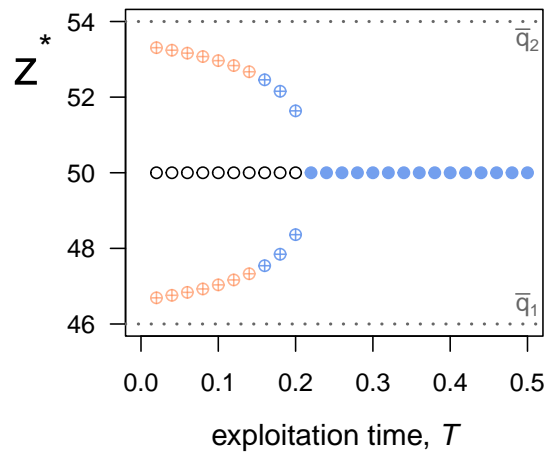


Figure S4: **Singular strategies and their stability under intermediate exploitation time T .** Bifurcation diagrams for singular strategies against exploitation time T (with $\sigma_g^2 = 3$, $\gamma = 0$, $n = 10$, $m = 0.8$, $\sigma_{r,w}^2 = 1$, and $\sigma_{r,b}^2 = 16$). White circles indicate singular strategies that are evolutionary repellers; crossed pink circles indicate singular strategies that are attractors and for which selection is stabilizing ($z_1^* = \bar{q} - \theta$ or $z_2^* = \bar{q} + \theta$); blue circles indicate singular strategies that are attractors and for which selection is disruptive, i.e., evolutionary branching points (solid: $z^* = \bar{q}$; crossed: $z_1^* = \bar{q} - \theta$ or $z_2^* = \bar{q} + \theta$). Dotted lines indicate the average resource property in each habitat, \bar{q}_1 and \bar{q}_2 . This shows that as exploitation time increases, polymorphism become more likely. This is because with longer exploitation time competition becomes more intense, favoring individuals to specialize on resources that are under less intense competition (eq. I.C in Box 1).

References

- Cotto, O., M. Schmid, and F. Guillaume. 2020. NEMO-AGE: Spatially explicit simulations of eco-evolutionary dynamics in stage-structured populations under changing environments. *Methods in Ecology and Evolution* 11:1227–1236.
- Dercole, F., and S. Rinaldi. 2008. *Analysis of Evolutionary Processes: The Adaptive Dynamics Approach and Its Applications*. Princeton University Press.
- Geritz, S. A. H., E. Kisdi, G. Meszéna, and J. A. J. Metz. 1998. Evolutionary singular strategies and the adaptive growth and branching of the evolutionary tree. *Evolutionary Ecology* 12:35–57.
- Goudet, J. 2005. HIERFSTAT, a package for R to compute and test hierarchical F-statistics. *Molecular Ecology Notes* 5:184–186.
- Karlin, S. 1968. Rates of approach to homozygosity for finite stochastic models with variable population size. *The American Naturalist* 102:443–455.
- Lehmann, L., C. Mullan, E. Akçay, and J. Van Cleve. 2016. Invasion fitness, inclusive fitness, and reproductive numbers in heterogeneous populations. *Evolution* 70:1689–1702.
- Martin, G., E. Chapuis, and J. Goudet. 2008. Multivariate Q_{ST} - F_{ST} comparisons: A neutrality test for the evolution of the G matrix in structured populations. *Genetics* 180:2135–2149.
- Metz, J. A. J., S. A. H. Geritz, G. Meszéna, F. J. A. Jacobs, and B. V. Heerwaarden. 1996. Adaptive dynamics, a geometrical study of the consequences of nearly faithful reproduction. Pages 183–231 in S. v. Strien and S. V. Lunel, eds. *Stochastic and spatial structures of dynamical systems*. Proceedings of the Royal Dutch Academy of Science, North Holland, Dordrecht, Netherlands.
- Ohtsuki, H., C. Rueffler, J. Y. Wakano, K. Parvinen, and L. Lehmann. 2020. The components of directional and disruptive selection in heterogeneous group-structured populations. *Journal of Theoretical Biology* 507:110449.
- R Core Team. 2019. *R: a language and environment for statistical computing*.
- Rousset, F. 2004. *Genetic Structure and Selection in Subdivided Populations*. Princeton University Press, Princeton and Oxford.
- Schmid, M., C. Rueffler, L. Lehmann, and C. Mullan. 2023. Data from: Resource variation within and between patches: Where exploitation competition, local adaptation and kin selection meet. *The American Naturalist*, FigShare, <https://doi.org/10.6084/m9.figshare.23617305>.
- Storz, J. F., J. Balasingh, H. R. Bhat, P. T. Nathan, D. P. S. Doss, A. A. Prakash, and T. H. Kunz. 2001. Clinal variation in body size and sexual dimorphism in an Indian fruit bat, *Cynopterus sphinx* (Chiroptera: Pteropodidae). *Biological Journal of the Linnean Society* 72:17–31.

Taylor, P. D. 1990. Allele-frequency change in a class-structured population. *The American Naturalist* 135:95–106.

Weir, B. S., and C. C. Cockerham. 1984. Estimating F-statistics for the analysis of population structure. *Evolution* 38:1358–1370.